# Inferring general links between energetics and information with unknown environment

Junjie Liu [1,2,*] Jincheng Lu [3] Chen Wang,[4] and Jian-Hua Jiang[5,6,7,†]

[1]*Department of Physics, International Center of Quantum and Molecular Structures, Shanghai University, Shanghai 200444, China*

[2]*Institute for Quantum Science and Technology, Shanghai University, Shanghai 200444, China*

[3]*Key Laboratory of Efficient Low-carbon Energy Conversion and Utilization of Jiangsu Provincial Higher Education Institutions, School of Physical Science and Technology, Suzhou University of Science and Technology, Suzhou 215009, China*

[4]*Department of Physics, Zhejiang Normal University, Jinhua, Zhejiang 321004, China*

[5]*School of Biomedical Engineering, Division of Life Sciences and Medicine, University of Science and Technology of China, Hefei 230026, China*

[6]*Suzhou Institute for Advanced Research, University of Science and Technology of China, Suzhou 215123, China*

[7]*Department of Modern Physics, School of Physical Sciences, University of Science and Technology of China, Hefei 230026, China*

(Received 3 June 2024; accepted 12 August 2024; published 21 August 2024)

Identifying general links between energetics and information in realistic open quantum systems is a long-standing problem in quantum thermodynamics and quantum information processing. However, the generality of existing efforts is often impeded by their specific assumptions about environments. Here we address the problem by developing a trajectory-level thermodynamic inference theory to establish general links using just the knowledge of the system, enabling a single framework applicable to a diverse range of environments. Underpinning the framework is a notion of excess energy introduced for inferring the net energy gain of the system after completing an information processing trajectory. We show that fluctuation behaviors of the excess energy encode general links between energetics and information with a conceptual advantage that they completely avoid *a priori* assumptions about environments and system-environment coupling forms. Crucially, we obtain a single thermodynamic inequality that integrates upper bounds on heat dissipation and extracted work in terms of system's information content change, providing complementary constraints that greatly expand the context of existing well-adopted results based on the second law of thermodynamics. We also uncover lower bounds on the precision of the fluctuating system's energy and information content changes in terms of their Fano factors and a correlation function between them. By extending relations between energetics and information to higher-order fluctuations, we thus reveal a trade-off that a more precise inference of energy or information content changes requires a looser energetic-information link. We showcase the implications of these general links in a number of quantum information and thermodynamic tasks of application relevance. Our framework provides a toolkit for analyzing the interplay between energetics and information from the trajectory level in generic quantum systems, thereby adding an indispensable structure to the thermodynamics of information.

DOI: 10.1103/PhysRevResearch.6.033202

## I. INTRODUCTION

Questing for the physical nature of information has led to profound insights into the understanding of information stored in both classical and quantum systems [1,2]. On the one hand, one can associate information which lacks a unique definition with meaningful operational interpretations [3–5], mapping it to an embodied physical entity that enables manipulation and transformation. A recent development that aligns with this research line focuses on quantum information engines [6–10] which build upon thermodynamic operations of information flows. On the other hand, information processing is generally carried out by dynamical systems [11], entangling information with physical observables of the information-bearing system. This promotes us to explore the physical nature of information in relation to physical observables. Since the seminal works in the context of Maxwell's demon [11], Szilard's engine [12], and Landauer's principle [13], understanding how thermodynamics and information intertwine in dynamical systems has become an established research area with renewable interests emerging at the intersection of quantum thermodynamics and quantum information [14,15].

Realistic dynamical systems are generally open and experience continuous changes in energy and information due to the coupling to surrounding environments [16]. Hence, identifying the energetic fingerprint of the information represents a natural goal to pursue towards a complete framework of the thermodynamics of information [15,17]. Along this line, the comprehension of quantum information processing has

*Contact author: jj_liu@shu.edu.cn

†Contact author: jhjiang3@ustc.edu.cn

recently brought up an intriguing problem of characterizing their associated energetic cost [18–20], with preliminary experimental attempts [21–23] being accomplished. It is now well appreciated that changes in the system's energy and von Neumann entropy which quantifies the information content of the system [24] are inherently linked [25,26], leading to thermodynamic constraints that information processing tasks should obey [11,13,26]. To establish relations between energetics and information, one usually assumes the environment to be thermal with a homogeneous temperature [15] so as to implement the second law of thermodynamics in a straightforward manner [26]. This basic thermal bath assumption underlies a notable number of theoretical extensions [27–42] and experimental investigations [43–49]. Despite the progress, a general formulation of the relation between energetics and information is still far from being achieved.

In many scenarios, the involved environment is not characterized by a single thermodynamic temperature, rendering the common assumption of a single thermal bath inapplicable. Notable examples include nonthermal environments [50–60] and dissipation-engineered reservoirs [61–67], which are routinely utilized as intriguing quantum resources in quantum thermodynamics and quantum information processing. In the absence of a homogeneous temperature, identifying the relations between energetics and information becomes intricate as it goes beyond the usual scope of the thermodynamics of information involving a single thermal bath [15,68]. To date, no general consensus has been reached regarding how to develop a description without invoking assumptions on temperatures or other information of environments so as to cover a wide range of contexts. Aiming for a complete solution, a desirable route would be conceiving relations between energetics and information that depend only on the system's observable degrees of freedom, which, however, remain vague.

Moreover, existing theoretical efforts have been largely devoted to relations between averaged values of energetic and information-theoretic quantities [27,28,31–40], missing their higher-order fluctuations which could encode extra information. In contrast, relevant experiments are usually preformed by collecting an ensemble of trajectories (see, e.g., Refs. [69,70]) and thus capable of extracting behaviors of not only averaged values but also higher-order fluctuations which can become significant in small quantum systems [69–72]. This discrepancy between experiment and theory emphasizes a need for theoretical tools building upon single trajectories which mimic the results of experiments.

Here we put forward a framework that is capable of satisfying the needs by offering a general strategy to link energetics and information from the trajectory level for systems coupled to environments of diverse types. To lift the conventional assumptions of knowing *ad hoc* details of environments and system-environment couplings, we frame the identification of intrinsic links as a problem of inference, where the actual relation between energetics and information is hidden and will be reconstructed given just the knowledge of the system. Reifying this inference perspective, we harness solely the system's dynamical information (e.g., time-dependent state and Hamiltonian) to introduce a notion of excess energy which underpins our framework. The excess energy connects the energetics and information of the system in a way that it quantifies the net energy gain of the system at the trajectory level by taking into account an energetic cost responsible for a change in system's information content enabled by thermodynamically inferred reference states.

Leveraging the techniques of stochastic thermodynamics [73,74], we obtain the cumulant generating function of the excess energy. We demonstrate that the fluctuation behaviors of the excess energy encode general links between energetics and information content of the system in forms of universal thermodynamic bounds which hold irrespective of details of the system, the environment, and their coupling. These bounds differ from existing ones exclusively derived from the second law of thermodynamics and thus serve as complementary descriptions. More importantly, these bounds have conceptual advantages that they can be sufficiently evaluated using only the dynamical information of the system which can be obtained from numerical simulations or experimental observations, and they cover a wide range of contexts, as Fig. 1(a) indicates.

Specifically, focusing on the first-order fluctuation of the excess energy, we reveal a single inequality that integrates intriguing upper bounds on averaged heat dissipation and extracted work from the dynamical system, which are two main energetic quantities of the system using the averaged system's information content change. From analyzing the second-order fluctuation of the excess energy, we also receive universal lower bounds on the precision of the fluctuating system's energy and information content changes in terms of their Fano factors and a correlation function between them, owing to a unique feature of the framework that fluctuations of energetic and information-theoretic quantities are treated to the same order. We remark that these lower bounds imply an intriguing trade-off relation that a more precise inference of energy or information content changes requires a looser energetic-information link. We thus extend relations between energetics and information to account for higher-order fluctuations. We exemplify these general thermodynamic links in a number of quantum thermodynamic and quantum information processing tasks covering a diversity of environments and contrast them with available existing results, highlighting the promising potential of our framework.

Our results are not only of theoretical interest, as we propose a systematic approach to treat the fluctuating system's energy and information content on equal footing, and add an additional structure to the collection of thermodynamic constraints on energetics and information [27,31–36,38,39,68], thereby greatly expanding the application range of the thermodynamics of information [15], but also of experimental relevance, as we provide a trajectory-level description which avoids accessing information of complex environments, thereby facilitating experimental implementations.

The paper is organized as follows. In Sec. II, we present our thermodynamic framework in detail. We first specify single trajectories in our consideration and define trajectory-level energetic and information-theoretic quantities of interest. We then introduce the notion of excess energy that underpins the framework by resorting to thermodynamically inferred reference states. We finally derive an analytical expression for the cumulant generating function of the excess energy. Then, in

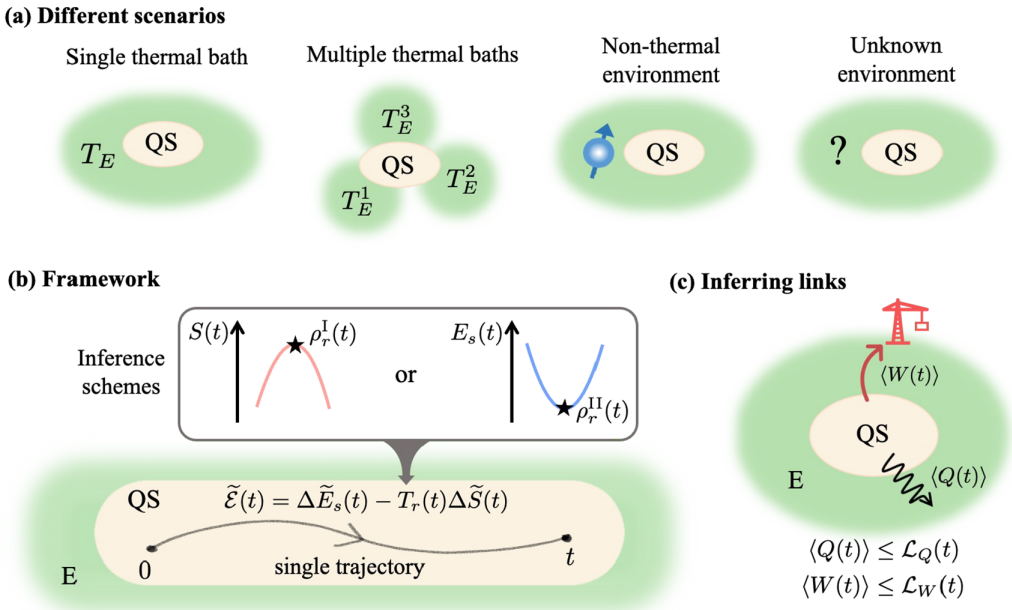


FIG. 1. Schematic of the study. (a) Open quantum systems (QS, orange shaded region) can couple to a diversity of environments (E, green shaded region), such as a single thermal bath with temperature $T_E$, multiple thermal baths with different temperatures, nonthermal environments, and even complex unknown environments whose detailed information remains inaccessible to measurement. (b) To understand the interplay between energetics and information in the scenarios shown in (a) with a unified viewpoint, we develop a general thermodynamic inference framework using the knowledge of the system only. Underpinning the framework is a notion of an excess energy $\widetilde{\mathcal{E}}(t)$ [Eq. (5)] which connects a trajectory-level system's energy change $\Delta\widetilde{E}_s(t)$ and a system's information content change $\Delta\widetilde{S}(t)$ through a parameter $T_r(t)$ inferred from solely system observables. We determine this parameter by developing two thermodynamic inference schemes to introduce a Gibbsian reference state $\rho_r^{\mathrm{I}}(t)$ [$\rho_r^{\mathrm{II}}(t)$] that has maximum von Neumann entropy $S^\star(t)$ or minimum information content [minimal energy $E_s^\star(t)$] over a surface of fixed energy $E_s(t)$ [fixed information content $S(t)$]; see details in Sec. II. (c) From analyzing fluctuation behaviors of the excess energy, we establish general links between energetics and information that apply to a wide range of scenarios, such as a single inequality integrating universal upper bounds $\mathcal{L}_Q(t)$ and $\mathcal{L}_W(t)$ on the averaged heat dissipation $\langle Q(t)\rangle$ and extracted work $\langle W(t)\rangle$ from the system with a contribution from the averaged system's information content change $\langle\Delta\widetilde{S}(t)\rangle$, respectively; see details in Sec. III.

Sec. III, we exploit the cumulant generating function of the excess energy to uncover universal links between energetics and information encoded in the fluctuation behaviors of the excess energy. We elaborate the distinct nature of obtained links by comparing them with their existing counterparts, which all require the knowledge of environments to some extent. To corroborate the promising potential of our framework, we examine these universal relations in Sec. IV by considering a number of representative quantum setups whose realizations are within current experimental capabilities, including a driven qubit system immersed in a single thermal bath used to implement a quantum information erasure process, a double quantum dot system coupled to two electronic and one phononic baths of different temperatures used for studying an inelastic heat transfer process, and a coupled Rydberg atom system used to realize a dissipative quantum state preparation process through dissipation engineering. We conclude the study in Sec. V with some final remarks. We set $\hbar \equiv 1$ and $k_B \equiv 1$ throughout this paper.

## II. THERMODYNAMIC FRAMEWORK

We now lay out our framework, as sketched in Fig. 1(b), that allows us to link energetics and information during a generic quantum process. The framework does not impose assumptions on the type of environments and thus applies to various setups, as Fig. 1(a) shows. We specify how to generate trajectories using a one-time measurement scheme [75–77] which imposes minimum measurement back-action on the system. We also define trajectory-level quantities of interest and introduce the notion of excess energy to quantify the net energy gain of the system after completing an information processing trajectory by exploiting thermodynamically inferred reference states. Finally, we present an analytical expression for the cumulant generating function of the fluctuating excess energy.

### A. Measurement, trajectory, and quantities

Without loss of generality, we consider an open quantum system described by a time-dependent Hamiltonian $H_s(t)$ whose spectrum is nondegenerate. The system undergoes a quantum evolution captured by a time-dependent reduced system density matrix $\rho_s(t)$. We thrive in establishing general relations between energetics and information of the system from the trajectory level by using solely the knowledge of $H_s(t)$ and $\rho_s(t)$, without further requiring knowledge of the environments.

We prepare single trajectories by adopting the one-time measurement scheme [75–77] in which one just performs an initial energy measurement on the system. Single trajectories are then obtained by evolving the measured eigenstates.

The quantum coherence generated during the evolution is preserved as compared with the two-time measurement scheme [73]. We stress that the trajectories we consider are distinct from the quantum jump ones introduced to stochastically unravel quantum master equations [78–80] and the classical ones describing Markov jump processes in stochastic thermodynamics [74]. To avoid initial measurement backaction, we require $[\rho_s(0), H_s(0)] = 0$, with $\rho_s(0)$ the initial system state before the measurement. A straightforward choice would be a Gibbsian initial state $\rho_s(0) = e^{-\beta_0 H_s(0)}/Z_0$ with $Z_0 = \mathrm{Tr}[e^{-\beta_0 H_s(0)}]$ and $\beta_0 = T_0^{-1} > 0$. We note that this form of initial state can be experimentally prepared through designed state-preparation algorithms [60,81]. Hence, $T_0$ is not necessarily a bath temperature.

Suppose at $t = 0$, the initial energy measurement selects an energy eigenstate $|\varepsilon_0\rangle$ of $H_s(0)$ with measurement outcome $\varepsilon_0$ and measurement probability $p_0 = e^{-\beta_0 \varepsilon_0}/Z_0$; $p_0$ varies between nondegenerate energy eigenstates. The evolved state for such a single trajectory reads $\widetilde{\rho}_s(t) = \mathcal{U}_t[|\varepsilon_0\rangle\langle\varepsilon_0|]$, with $\mathcal{U}_t$ a completely positive trace-preserving map which is the same for every trajectory. By definition, the ensemble average $\langle\widetilde{\rho}_s(t)\rangle$ reproduces the evolved full state $\rho_s(t) = \mathcal{U}_t[\rho_s(0)]$ due to the linearity of the quantum channel $\mathcal{U}_t$. Throughout the paper, we use the notation $\widetilde{\mathcal{O}}$ to mark an arbitrary quantity at the trajectory level and denote its ensemble average as $\langle\widetilde{\mathcal{O}}\rangle \equiv \sum_{p_0} p_0 \widetilde{\mathcal{O}}$, which is evaluated over the complete set of initial measurement probabilities $\{p_0\}$ whose number of elements depends on the dimension of the system Hamiltonian.

We introduce a microscopic energy change at the trajectory level [76]:

$$\Delta\widetilde{E}_s(t) \equiv \widetilde{E}_s(t) - \varepsilon_0. \tag{1}$$

Here, we have denoted $\widetilde{E}_s(t) = \mathrm{Tr}[H_s(t)\widetilde{\rho}_s(t)]$ as the internal energy of the system along a single trajectory. We remark that $\langle\Delta\widetilde{E}_s(t)\rangle = \mathrm{Tr}[H_s(t)\rho_s(t)] - \mathrm{Tr}[H_s(0)\rho_s(0)]$, with $\langle\varepsilon_0\rangle = \mathrm{Tr}[H_s(0)\rho_s(0)]$, namely, the ensemble average $\langle\Delta\widetilde{E}_s(t)\rangle$ of $\Delta\widetilde{E}_s(t)$ recovers the correct expectation value of the system's energy change during the full quantum process of $\rho_s(0) \to \rho_s(t)$.

As for the information-theoretic quantity of interest, we focus on the information content of the system. In this regard, we notice that the von Neumann entropy quantifies the number of qubits needed to store the information encoded in the system state [82], in a way similar to the Shannon entropy for classical systems. We hence follow the convention in the quantum information theory by adopting the von Neumann entropy as the measure for the information content of the system [24]. Accordingly, we refer to a change in the von Neumann entropy as a change in information content hereafter. To ensure that the correct value of the system's information content change $S(t) - S(0)$ with $S(t) = -\mathrm{Tr}[\rho_s(t)\ln\rho_s(t)]$ during the full process can be recovered, we identify

$$\Delta\widetilde{S}(t) \equiv -\mathrm{Tr}[\widetilde{\rho}_s(t)\ln\rho_s(t)] + \ln p_0 \tag{2}$$

as the microscopic system's information content change at the trajectory level. It can be readily checked that $\langle\Delta\widetilde{S}(t)\rangle = S(t) - S(0)$. On the contrary, the system's information content change $\widetilde{S}(t) - \widetilde{S}(0)$ with $\widetilde{S}(t) = -\mathrm{Tr}[\widetilde{\rho}_s(t)\ln\widetilde{\rho}_s(t)]$ during a single trajectory of $|\varepsilon_0\rangle\langle\varepsilon_0| \to \widetilde{\rho}_s(t)$ does not recover the correct expectation value, namely, $\langle\widetilde{S}(t) - \widetilde{S}(0)\rangle \neq S(t) - S(0)$. We point out that the definition $\Delta\widetilde{S}(t)$ in Eq. (2) preserves the quantum coherence generated during the evolution, as we use density matrices instead of probabilities at finite times. When the quantum coherence vanishes completely during the evolution as in the case of a Markov jump process, both $\widetilde{\rho}_s(t)$ and $\rho_s(t)$ become diagonal in the energy basis. In this special scenario, suppose the system reaches one of energy eigenstates $|\varepsilon_t\rangle$ at time $t$ during a single trajectory—one finds $\Delta\widetilde{S}(t) = -\ln p_t + \ln p_0$ with $p_t = \langle\varepsilon_t|\rho_s(t)|\varepsilon_t\rangle$, which is just the frequently used definition for trajectory-level entropy production in stochastic thermodynamics [74].

### B. Thermodynamic inference schemes and reference states

We aim to link $\Delta\widetilde{E}_s(t)$ and $\Delta\widetilde{S}(t)$ defined in the above subsection. From a dimensional analysis, we note that $\Delta\widetilde{E}_s(t)$ and $\Delta\widetilde{S}(t)$ can be transformed into quantities of the same dimension once we invoke a parameter of the same dimension as the thermodynamic temperature. By considering an isothermal setup involving a single thermal bath, Refs. [75,76] introduced a thermal state by maximizing the von Neumann entropy of the system-bath composite system [83]. They utilized this thermal state as a reference point for evaluating thermodynamic quantities to have a thermodynamic description that is compatible with the one-time measurement scheme. However, since we avoid making the assumption of a single thermal bath, we cannot define a reference thermal state with a thermodynamic temperature.

In light of recent refinements of the notion of reference states in the studies of quantum thermodynamics [39,84–89], we instead introduce a thermodynamic inference scheme in which one infers a reference state $\rho_r(t)$ from solely measurable system observables. The reference state $\rho_r(t)$ we consider does not need to have a meaningful thermodynamic interpretation but rests its foundation in experimental observations on system observables. The dimensional requirement promotes us to consider a reference state of the Gibbsian form $\rho_r(t) = e^{-\beta_r(t)H_s(t)}/Z_r(t)$, with $Z_r(t) = \mathrm{Tr}[e^{-\beta_r(t)H_s(t)}]$ determined by a single time-dependent parameter $\beta_r(t)$. To bridge the Gibbsian reference state or, equivalently, the single parameter $\beta_r(t)$ and system observables, we recall the intriguing properties of a Gibbsian state, that it possesses minimum energy (information content) among states of the same dimension and information content (energy). For the sake of completeness, we relegate details of the proof to Appendix A.

Given the aforementioned features of a Gibbsian state, we then summarize two single-parameter inference schemes by exploiting the knowledge of the system state and Hamiltonian only. The first inference scheme, which we dub an equal-energy one, yields a Gibbsian reference state $\rho_r^{\mathrm{I}}(t)$ with minimum information content (maximum von Neumann entropy) under the fixed energy constraint (time dependence is suppressed for simplicity):

$$\rho_r^{\mathrm{I}}: \max_{\rho_r}[S(\rho_r)]|_{\mathrm{Tr}(H_s\rho_r)=\langle\widetilde{E}_s\rangle}. \tag{3}$$

Here, $S(\rho_r(t)) = -\mathrm{Tr}[\rho_r(t)\ln\rho_r(t)]$ denotes the von Neumann entropy of an arbitrary state $\rho_r(t)$ living in the system Hilbert space. The energy of state $\rho_r(t)$ is fixed by the system actual averaged energy $\langle\widetilde{E}_s(t)\rangle$. The alternative inference

scheme, which we dub an equal-information-content one, amounts to identifying a Gibbsian reference state $\rho_r^{\rm II}(t)$ that yields minimal averaged energy $\mathrm{Tr}[H_s(t)\rho_r(t)]$ among states with the same information content fixed by $S(t)$ of $\rho_s(t)$ (time dependence is suppressed for simplicity):

$$\rho_r^{\rm II}: \min_{\rho_r}[\mathrm{Tr}(H_s\rho_r)]|_{S(\rho_r)=S}. \tag{4}$$

These two single-parameter inference schemes can be efficiently implemented subject to numerical simulations or experimental observations on the system. Notably, we obtain Gibbsian reference states by using the full system dynamics such that they are equally applicable for all trajectories. Moreover, they provide unbiased single reference points as they reflect extreme values of the energy and information content that the system can attain under the given constraints. We stress that the existence of Gibbsian reference states does not imply the system stays in a true thermal equilibrium state. Despite its virtual nature, the Gibbsian reference state can find its relevance in information-preserving and energy-preserving operations on the system [87].

Specifically, the single parameter $\beta_r(t)$ of the Gibbsian reference states $\rho_r^{\rm I}(t)$ and $\rho_r^{\rm II}(t)$ can be determined by invoking the equal-energy condition $\mathrm{Tr}[H_s(t)\rho_r^{\rm I}(t)] = \langle\widetilde{E}_s(t)\rangle$ and the equal-information-content condition $S[\rho_r^{\rm II}(t)] = S(t)$, respectively. Hence, we relate the inferred parameter $\beta_r(t)$ with measurable quantities, thereby laying an experimental basis for inferring a Gibbsian reference state. We note that $\beta_r(t)$ obtained using the latter condition was referred to as an intrinsic temperature of the system by Ref. [87]. However, we avoid such a nomenclature here and treat $\beta_r(t)$ just as an inferred parameter from the knowledge of the system since the reference state is virtual, in general. With the initial Gibbsian state $\rho_s(0)$ introduced before, both inference schemes predict $\rho_r^{\rm I,II}(0) = \rho_s(0)$ with $\beta_r^{\rm I}(0) = \beta_r^{\rm II}(0) = \beta_0$. At finite times, we expect $\rho_r^{\rm I}(t) \neq \rho_r^{\rm II}(t)$ [or, equivalently, $\beta_r^{\rm I}(t) \neq \beta_r^{\rm II}(t)$], in general, as the actual full state $\rho_s(t)$ can deviate from a Gibbsian form such that the averaged internal energy and information content of the system could yield distinct inferences for the single parameter $\beta_r(t)$. An exception is a quasistatic isothermal process where we always have $\rho_r^{\rm I}(t) = \rho_r^{\rm II}(t)$ since the system stays in an instantaneous thermal state.

### C. Excess energy

Noting the dimension of the inferred parameter $T_r(t) \equiv \beta_r^{-1}(t)$ and previously defined trajectory-level quantities, we are ready to introduce a notion dubbed excess energy $\widetilde{\mathcal{E}}(t)$, which plays a vital role in linking energetics and information within our framework:

$$\widetilde{\mathcal{E}}(t) \;\equiv\; \Delta\widetilde{E}_s(t) - T_r(t)\Delta\widetilde{S}(t). \tag{5}$$

Crucially, this quantity involves only the system's dynamical information. To elaborate the physical meaning of the excess energy, we recall that for quasistatic isothermal processes the inferred parameter $T_r(t)$ is fixed by the environment temperature $T_E$. Therefore, in this scenario the ensemble average $T_r(t)\langle\Delta\widetilde{S}(t)\rangle = T_E\langle\Delta\widetilde{S}(t)\rangle$ recovers exactly the bound on energetic cost in the context of the Landauer's principle [13,25,89]. We thus interpret the term $T_r(t)\Delta\widetilde{S}(t)$ in Eq. (5) generally as an inferred energetic cost paid to increase the system's information content by an amount of $\Delta\widetilde{S}(t)$ during an arbitrary process. As $\Delta\widetilde{E}_s(t)$ denotes a system's energy gain, the excess energy $\widetilde{\mathcal{E}}(t)$ as a whole then functions as a quantifier for the net energy gain of the system after completing an information processing trajectory with a change in the information content. We emphasize that the notion of excess energy has no existing counterparts. In particular, we point out that the excess energy does not equal a change in a generalized nonequilibrium free energy $\widetilde{\mathcal{F}}(t) = \widetilde{E}_s(t) - T_r(t)\widetilde{S}(t)$ of the system along a single trajectory [89] since $\Delta\widetilde{S}(t) \neq \widetilde{S}(t) - \widetilde{S}(0)$ in Eq. (2). We also note that the excess energy is unbounded by the second law of thermodynamics. Therefore, the excess energy provides an independent perspective for the understanding of energetic fingerprint of information processing [20] from the trajectory level.

In addition, the excess energy includes the system's energetic and information-theoretic quantities with the same order, allowing us to treat the fluctuations of energetics and information on equal footing. With this conceptual advance, we are able to uncover distinct links between energetics and information that complement and extend existing results by just analyzing the fluctuation behavior of the excess energy (see Sec. III). We finally remark that the excess energy defined in Eq. (5) remains form invariant for the two inference schemes. However, the two inference schemes would yield different values for the parameter $T_r(t)$ as well as the excess energy in detailed models. We can thus contrast the performance of the two inference schemes and select the tighter one in specific scenarios, as we will show in Sec. IV.

### D. Cumulant generating function

We resort to the cumulant generating function [73] to describe the fluctuation behavior of the excess energy. To this end, we introduce a counting field $\chi$ and consider the scaled fluctuating quantity $\beta_r(t)\widetilde{\mathcal{E}}(t)$ [recall that the parameter $\beta_r(t)$ does not fluctuate between trajectories by its definition]. We then define the corresponding cumulant generating function of $\beta_r(t)\widetilde{\mathcal{E}}(t)$ as $G(\chi,t) \equiv \ln\langle\exp[-\chi\beta_r(t)\widetilde{\mathcal{E}}(t)]\rangle$ [73].

We aim to derive an expression for the cumulant generating function $G(\chi,t)$ that is amenable to analytical and numerical treatments. We first note that the trajectory-level energy change defined in Eq. (1) can be reexpressed as $\Delta\widetilde{E}_s(t) = T_r(t)\widetilde{S}(t) + \widetilde{\mathcal{F}}(t) - \varepsilon_0$ by using the generalized nonequilibrium free energy introduced below Eq. (5). We then have $\beta_r(t)\widetilde{\mathcal{E}}(t) = -D[\widetilde{\rho}_s(t)||\rho_s(t)] + \beta_r(t)\widetilde{\mathcal{F}}(t) - \beta_r(t)\varepsilon_0 - \ln p_0$, with $D(\rho_1||\rho_2) = \mathrm{Tr}[\rho_1(\ln\rho_1 - \ln\rho_2)]$ denoting the quantum relative entropy between two states $\rho_{1,2}$. To proceed, we utilize an information-theoretic expression for the nonequilibrium free energy $\widetilde{\mathcal{F}}(t) = -T_r(t)\ln Z_r(t) + T_r(t)D(\widetilde{\rho}_s(t)||\rho_r(t))$ [89,90] to rewrite $\beta_r(t)\widetilde{\mathcal{E}}(t) = \mathrm{Tr}\{\widetilde{\rho}_s(t)\ln[\rho_s(t)/\rho_r(t)]\} - \ln Z_r(t) - \beta_r(t)\varepsilon_0 - \ln p_0$. Finally, we arrive at the following expression for the cumulant generating function $G(\chi,t)$:

$$G(\chi,t) = \chi\ln Z_r(t) + \ln\langle\exp[\chi\widetilde{\mathcal{B}}(t)]\rangle. \tag{6}$$

Here, we have denoted $\widetilde{\mathcal{B}}(t) \equiv -\mathrm{Tr}\{\widetilde{\rho}_s(t)\ln[\rho_s(t)/\rho_r(t)]\} + \beta_r(t)\varepsilon_0 + \ln p_0$, which determines higher-order fluctuations of the excess energy, as will be seen. The $n$th order cumulant $\langle\langle[\beta_r(t)\widetilde{\mathcal{E}}(t)]^n\rangle\rangle$ of $\beta_r(t)\widetilde{\mathcal{E}}(t)$ reads $\langle\langle[\beta_r(t)\widetilde{\mathcal{E}}(t)]^n\rangle\rangle \equiv$

$(-1)^n \partial_\chi^n G(\chi, t)|_{\chi=0}$. In the following, we will resort to the cumulant generating function $G(\chi, t)$ to establish links between energetic and information-theoretical quantities.

## III. UNIVERSAL LINKS BETWEEN ENERGETICS AND INFORMATION

In this section, by using the cumulant generating function of the excess energy given in Eq. (6), we show that the fluctuation behaviors of the excess energy encode universal links between energetics and information in forms of intriguing thermodynamic inequalities. We also highlight the distinct aspects of these links as compared with existing ones.

### A. Integrated thermodynamic upper bound on heat dissipation and extracted work

We first focus on the first-order cumulant, or, equivalently, the mean of the excess energy $\langle \beta_r(t)\widetilde{\mathcal{E}}(t)\rangle$. Using the cumulant generating function in Eq. (6), we find $-\langle \beta_r(t)\widetilde{\mathcal{E}}(t)\rangle = \ln Z_r(t) + \langle \widetilde{\mathcal{B}}(t)\rangle$. Since $\langle \mathrm{Tr}\{\widetilde{\rho}_s(t)\ln[\rho_s(t)/\rho_r(t)]\}\rangle = D[\rho_s(t)||\rho_r(t)]$ and $\langle \ln p_0\rangle = -\beta_0\langle \varepsilon_0\rangle - \ln Z_0$ in $\langle \widetilde{\mathcal{B}}(t)\rangle$, we arrive at the following universal inequality as a result of the non-negative nature of the quantum relative entropy:

$$\beta_0\langle \Delta\widetilde{E}_s(t)\rangle - \langle \Delta\widetilde{S}(t)\rangle + \ln\frac{Z_r(t)}{Z_0} + \Delta\beta_r(t)\langle \widetilde{E}_s(t)\rangle \geqslant 0. \tag{7}$$

Here, we have denoted $\Delta\beta_r(t) \equiv \beta_r(t) - \beta_0$. Noting this inequality only demands that an initial Gibbsian state with $\beta_0$ be defined, and no restrictions on the actual full state $\rho_s(t)$ at later times are needed. $\rho_s(t)$ can deviate from a Gibbsian form during the evolution. Indeed, for any meaningful information processing, the system must undergo a nonequilibrium process [11,15]. We also stress that the above inequality holds regardless of the dynamical details of the system and, particularly, remains form invariant for the two inference schemes which start to take effect when evaluating the last two terms on the left-hand side of Eq. (7) for detailed processes. Remarkably, when determining the parameter $\beta_r(t)$ using the equal-information-content inference scheme, Eq. (7) subsumes a previous result in Ref. [89]. However, we point out that Eq. (7) rests its origin in the first-order fluctuation of the excess energy whereas such a microscopic picture is missed in Ref. [89]. In the following, we provide a thorough assessment of Eq. (7) to release its full potential.

Intriguingly, we will show that Eq. (7) integrates universal upper bounds on averaged heat dissipation $\langle Q(t)\rangle$ and extracted work $\langle W(t)\rangle$ from the system, which are often addressed separately in the existing literature. With just the knowledge of the system, we adopt definitions $\langle Q(t)\rangle \equiv -\int_0^t \mathrm{Tr}[H_s(\tau)\dot{\rho}_s(\tau)]d\tau$ [35] and $\langle W(t)\rangle \equiv -\int_0^t \mathrm{Tr}[\rho_s(\tau)\dot{H}_s(\tau)]d\tau$ [91], with $\dot{\mathcal{O}} \equiv d\mathcal{O}/dt$. We then receive a decomposition $\langle \Delta\widetilde{E}_s(t)\rangle = -\langle Q(t)\rangle - \langle W(t)\rangle$ which, together with Eq. (7), yield the following upper bounds applicable for both isothermal and nonisothermal processes:

$$\begin{aligned} \langle Q(t)\rangle &\leqslant \mathcal{L}_Q(t), \\ \langle W(t)\rangle &\leqslant \mathcal{L}_W(t), \end{aligned} \tag{8}$$

where

$$\mathcal{L}_Q(t) \equiv T_0\left[-\langle \Delta\widetilde{S}(t)\rangle + \ln\frac{Z_r(t)}{Z_0} + \Delta\beta_r(t)\langle \widetilde{E}_s(t)\rangle\right] - \langle W(t)\rangle, \tag{9}$$

and $\mathcal{L}_W(t)$ is obtained by switching $W$ and $Q$ in the above equation. The bounds are agnostic with respect to the knowledge of environment and can be sufficiently evaluated using just the system state and Hamiltonian. We infer from the similar forms between $\mathcal{L}_{Q,W}(t)$ that upper bounds on averaged heat dissipation and extracted work from the system are intrinsically connected with a common contribution shown in the first line of Eq. (9). As for the quantity in the second line of Eq. (9), we notice that it requires the same information as the bounded quantity to evaluate. This redundancy, originating from the energy decomposition, in fact, reflects a key feature of statistical inference using a limited set of observed data: the same data that supplies an estimate (averaged value of a quantity) can also access its accuracy (bound). Therefore, our bounds align with the inference consideration and reveal intriguing links between energy and information that are impossible with the second law of thermodynamics. Notably, $\langle Q(t)\rangle$ and $\langle W(t)\rangle$ can take negative values, which simply means that one should instead inject heat and work into the system so as to complete the process. Nevertheless, the upper bounds in Eq. (8) remain valid regardless of the sign of $\langle Q(t)\rangle$ and $\langle W(t)\rangle$. In Sec. IV, we will use superscripts I and II to discriminate upper bounds with $\beta_r(t)$ evaluated using the equal-energy and equal-information-content inference scheme, respectively.

To evaluate the thermodynamic significance and application range of the bounds in Eq. (8), it is desirable to elaborate the adopted definitions on heat and work in relation to the conventional ones which involve information of environments and system-environment couplings [26,27,91]. We note that for scenarios where only the system is being driven, the work definition adopted here is just the conventional one [27,91]. Hence, the work bound $\mathcal{L}_W(t)$ can be applied to arbitrary thermodynamic conditions. In contrast, we stress that the definition $\langle Q(t)\rangle$ equals the conventional one, which defines heat as the energy change of a thermal bath [26,27,91] only in a single bath scenario with weak system-bath couplings. Strictly speaking, $\langle Q(t)\rangle$ may no longer adopt a thermodynamic interpretation of heat beyond the weak coupling limit [92]. Therefore, when interpreting $\langle Q(t)\rangle$ as a thermodynamic heat, the upper bound $\mathcal{L}_Q(t)$ can only be applied to the weak coupling regime. Nevertheless, $\langle Q(t)\rangle$, being the complement of $-\langle \Delta\widetilde{E}_s(t)\rangle - \langle W(t)\rangle$ according to the first law of thermodynamics, is still a valid thermodynamic quantity at arbitrary coupling strength and with arbitrary number of baths. With this in mind, one can study its behaviors including the associated upper bound also under arbitrary thermodynamic conditions. More crucially, when one just has access to system degrees of freedom as we emphasize here, the current definition $\langle Q(t)\rangle$ is the only option to study the heatlike contribution to energetics.

It is worth contrasting bounds in Eq. (8) with existing results which are exclusively based on the second law of thermodynamics, thereby highlighting the distinct nature of our framework. We first focus on the isothermal process in

which the system couples to a single thermal bath of temperature $T_E$ since a great number of existing results focused on this special scenario. Before proceeding, it is worth stressing that $T_0$ appearing in the bounds $\mathcal{L}_{Q,W}(t)$ just determines the initial system Gibbsian state and can be independent of the bath temperature $T_E$ since $T_0$ can remain nonzero even when $T_E \to 0$ (see Ref. [39] for an example). For the moment, we consider finite $T_E$ and set $T_0 = T_E$ in $\mathcal{L}_{Q,W}(t)$ to facilitate comparisons, which amounts to preparing the initial Gibbsian state by directly attaching the system to the thermal bath instead of using bath-independent state-preparation algorithms [60,81]. We will discuss the nonisothermal scenario and the zero temperature limit of $T_E \to 0$ at the end of this subsection in which we treat $T_0$ and $T_E$ independently, emphasizing the distinction between $T_0$ and $T_E$ there.

For the heat dissipation, when limiting ourselves to weak system-bath couplings and a single thermal bath scenario, we can compare the bound $\mathcal{L}_Q(t)$ with the well-adopted Landauer's principle, $\langle Q(t)\rangle \geqslant -T_E\langle\Delta\widetilde{S}(t)\rangle$, which is directly related to the second law of thermodynamics [26]. We clearly observe that $\mathcal{L}_Q(t)$ contains the same contribution $-T_E\langle\Delta\widetilde{S}(t)\rangle$. However, besides this common contribution from the state function change, $\mathcal{L}_Q(t)$ also includes extra contributions from state-dependent and process-dependent quantities as manifested by the last three terms on the right-hand side of Eq. (9). With these extra contributions, $\mathcal{L}_Q(t)$ is capable of capturing the dynamical information over the course of the process (such as whether the system is being driven and out of equilibrium) that is, however, missed in Landauer's principle. We thus expect a tight performance of $\mathcal{L}_Q(t)$ at finite times as compared with Landauer's principle. In this regard, we note that improving the finite-time performance of Landauer's principle also relies on process-dependent correction terms [34,35,93].

As for the extracted work, we particularly contrast the bound $\mathcal{L}_W(t)$ with an existing upper one $-\Delta F(t) - T_E\Delta S_m$ obtained from a generalized second law of thermodynamics [94,95]. For later convenience, we dub $-\Delta F(t) - T_E\Delta S_m$ the second-law work bound by noting that the upper bound $\mathcal{L}_W(t)$ is derived without resorting to the second law of thermodynamics. In the expression of the second-law work bound, $\Delta F(t) = -T_E\ln[Z_0(t)/Z_0]$ denotes the change in the Helmholtz free energy of the system between the final and initial thermal equilibrium states with $Z_0(t) = \mathrm{Tr}[e^{-H_s(t)/T_E}]$ and $Z_0 \equiv Z_0(0)$, and $\Delta S_m$ is the system's von Neumann entropy change induced by quantum measurements [95]. The second-law work bound subsumes several well-known scenarios: For a cyclic isothermal feedback control process implemented in a two-state system, the second-law work bound approaches the Szilard limit $T_E\ln 2$ as $\Delta F(t) = 0$ and $\Delta S_M = -\ln 2$ [28,96]. For isothermal processes without measurements, the second-law work bound reduces to the classical free-energy bound $-\Delta F(t)$.

We observe that our upper bound $\mathcal{L}_W(t)$ contains contributions $T_E\ln[Z_r(t)/Z_0] - T_E\langle\Delta\widetilde{S}(t)\rangle$ that resemble those in the second-law work bound (recall that we set $T_0 = T_E$ to facilitate comparisons). Particularly, $\langle\Delta\widetilde{S}(t)\rangle$ can equal $\Delta S_m$ if one considers a measurement process. Still, the two work bounds are distinct. Not to mention additional contributions $T_E\Delta\beta_r(t)\langle\widetilde{E}_s(t)\rangle - \langle Q(t)\rangle$ to $\mathcal{L}_W(t)$ that are absent in the second-law work bound, we would also like to point out that $Z_r(t)$ in $\mathcal{L}_W(t)$ that is determined using thermodynamic inference schemes does not necessarily equal $Z_0(t)$ appearing in the second-law work bound at finite times, noting that the dynamical evolution of the system can deviate from the instantaneous thermal equilibrium path of the isothermal process which renders $T_r(t) \neq T_E$. We then expect that the bound $\mathcal{L}_W(t)$ can capture emergent nonequilibrium features during a finite-time isothermal evolution as $Z_r(t)$ is inferred using the actual nonequilibrium state $\rho_s(t)$. In the quasistatic limit where $Z_r(t)$ and $Z_0(t)$ equal and $\Delta\beta_r(t) = 0$, the bound $\mathcal{L}_W(t)$ is still distinct from the second-law work bound as the former involves a contribution from the averaged heat dissipation which compensates the contribution $-T_E\langle\Delta\widetilde{S}(t)\rangle$ according to Landauer's principle.

Going beyond the isothermal process, the Landauer bound and the second-law work bound mentioned above become immediately inapplicable as a single bath temperature $T_E$ becomes ill-defined, whereas the bounds $\mathcal{L}_{Q,W}(t)$ obtained herein remain valid as they are based solely on knowledge of the system. In this scenario, we remark that the parameter $\beta_r(t)$ (including $\beta_0$) in $\mathcal{L}_{Q,W}(t)$ is no longer associated with a thermodynamic interpretation even in the quasistatic limit and, particularly, $T_0$ in Eq. (9) cannot be identified as a bath temperature anymore. To evaluate the upper bounds for nonisothermal processes, we first infer the parameter $\beta_r(t)$ using either the averaged internal energy or the averaged information content of the system and then utilize the inferred parameter together with the system's dynamical information to calculate the involved terms in Eq. (9).

Lastly, we address a special scenario of undriven quantum systems undergoing an arbitrary evolution where the extracted work due to external driving fields vanishes. We emphasize that the upper bound $\mathcal{L}_Q(t)$ in Eq. (9) obtained from using a time-dependent Gibbsian reference state remains applicable in this scenario. Nevertheless, we remark that undriven systems also allow for a time-independent Gibbsian reference state $\rho_r = e^{-\beta_r H_s}/Z_r$ due to a time-independent Hamiltonian $H_s$. The corresponding time-independent parameter $\beta_r$ can be sufficiently inferred using either the initial internal energy $\langle\widetilde{E}_s(0)\rangle$ or the initial information content $S(0)$ of undriven systems, all yielding $\beta_r = \beta_0$. In doing so, we arrive at a simplified upper bound on averaged heat dissipation valid for undriven systems:

$$\mathcal{L}_Q^{\mathrm{un}}(t) = -T_0\langle\Delta\widetilde{S}(t)\rangle. \tag{10}$$

It is evident that the two thermodynamic inference schemes could yield the same prediction for $\mathcal{L}_Q^{\mathrm{un}}(t)$. We stress that using initial conditions which are known *a priori* by the one-time measurement scheme to fix $\rho_r$ is just a straightforward and simple option. It does not mean that the time-independent reference state can only be applied at the initial time. In fact, one can certainly use dynamical information at a finite time point to infer $\beta_r$ at the cost of a more complex bound compared with Eq. (10). Here we just limit ourselves to Eq. (10) for simplicity. The simple form of $\mathcal{L}_Q^{\mathrm{un}}(t)$ resembles that of the Landauer bound $-T_E\langle\Delta\widetilde{S}(t)\rangle$. However, being a valid upper bound for undriven systems, we should point out that $\mathcal{L}_Q^{\mathrm{un}}(t)$ is distinct from the Landauer lower bound even in the validity

regime of the latter, where a single bath temperature $T_E$ can be defined. Particularly, $\mathcal{L}_Q^{\rm un}(t)$ can remain nonzero in the zero-temperature limit of $T_E \to 0$, unlike the Landauer bound [39].

To clarify the above statement, remember that the parameter $T_0$ in Eq. (10) that determines the initial system Gibbsian state is independent of the bath temperature $T_E$. Considering heat dissipation in a two-level system due to spontaneous emission [39], $T_0$ is in one-to-one correspondence with an initial excitation probability of the two-level system. To have nonzero heat dissipation even in the limit of $T_E \to 0$ for a two-level system [97], one requires a nonzero initial excitation probability regardless of bath temperature $T_E$ [39]. Hence, we deduce that the parameter $T_0$ and, consequently, the bound $\mathcal{L}_Q^{\rm un}(t)$ can remain nonzero as we take the limit of $T_E \to 0$. In contrast, the Landauer bound tends to zero in this limit, highlighting the distinction between $\mathcal{L}_Q^{\rm un}(t)$ and the Landauer bound. Following this argument, we know that the full upper bound $\mathcal{L}_Q(t)$ should also remain nontrivial in the limit of $T_E \to 0$. We note that Ref. [39] obtained a lower bound on heat dissipation with a nontrivial zero temperature limit for undriven systems by assigning a Gibbsian reference state to the environment, thereby requiring the dynamical knowledge of the evolved bath state to evaluate the bound. In comparison, we obtain the bound $\mathcal{L}_Q^{\rm un}(t)$ by assigning a Gibbsian reference state to the system. Thus, we just need the dynamical knowledge of the system to evaluate $\mathcal{L}_Q^{\rm un}(t)$, which is computationally and experimentally easier to obtain than that of the environment.

### B. Thermodynamic lower bound on precision

We now turn to second-order fluctuation of the excess energy in light of recent interest in the thermodynamic uncertainty relation [98–100]. We first note the following Cauchy-Schwarz inequality (time dependence is suppressed in this subsection for simplicity):

$$\langle(\Delta\widetilde{E}_s - \langle\Delta\widetilde{E}_s\rangle)(\beta_r\widetilde{\mathcal{E}} - \langle\beta_r\widetilde{\mathcal{E}}\rangle)\rangle^2 \leqslant \mathrm{Var}(\Delta\widetilde{E}_s)\mathrm{Var}(\beta_r\widetilde{\mathcal{E}}). \tag{11}$$

Here, $\mathrm{Var}(\mathcal{O}) \equiv \langle\mathcal{O}^2\rangle - \langle\mathcal{O}\rangle^2$ denotes the variance (second-order cumulant) of $\mathcal{O}$. The equality is taken only when there exists a nonzero constant $\lambda$ such that $\Delta\widetilde{E}_s - \langle\Delta\widetilde{E}_s\rangle = \lambda(\beta_r\widetilde{\mathcal{E}} - \langle\beta_r\widetilde{\mathcal{E}}\rangle)$. However, this condition can hardly be met in the present study due to a nonzero contribution from $\Delta\widetilde{S} - \langle\Delta\widetilde{S}\rangle$ to the first-order fluctuation of the excess energy $\beta_r\widetilde{\mathcal{E}} - \langle\beta_r\widetilde{\mathcal{E}}\rangle$. That being said, the inequality Eq. (11) can become rather tight when the contribution $\beta_r(\Delta\widetilde{E}_s - \langle\Delta\widetilde{E}_s\rangle)$ prevails in the first-order fluctuation $\beta_r\widetilde{\mathcal{E}} - \langle\beta_r\widetilde{\mathcal{E}}\rangle$.

Using the definition in Eq. (5), we find $\langle(\Delta\widetilde{E}_s - \langle\Delta\widetilde{E}_s\rangle)(\beta_r\widetilde{\mathcal{E}} - \langle\beta_r\widetilde{\mathcal{E}}\rangle)\rangle = \beta_r\mathrm{Var}(\Delta\widetilde{E}_s) - \mathrm{Cor}(\Delta\widetilde{E}_s, \Delta\widetilde{S})$, with $\mathrm{Cor}(\mathcal{O}_1, \mathcal{O}_2) \equiv \langle\mathcal{O}_1\mathcal{O}_2\rangle - \langle\mathcal{O}_1\rangle\langle\mathcal{O}_2\rangle$ denoting a correlation function between two quantities $\mathcal{O}_{1,2}$. From the cumulant generating function in Eq. (6), we obtain the variance $\mathrm{Var}(\beta_r\widetilde{\mathcal{E}}) = \mathrm{Var}(\widetilde{\mathcal{B}})$. We can interpret $\mathrm{Var}(\widetilde{\mathcal{B}})$ as an indicator for characterizing the energetic stability, or constancy, for completing an information processing process. Then we can transform Eq. (11) into a universal lower bound on the precision $\mathrm{Var}(\Delta\widetilde{E}_s)/\langle\Delta\widetilde{E}_s\rangle^2$ [98] in terms of the Fano factor $\mathrm{Var}(\Delta\widetilde{E}_s)/\langle\Delta\widetilde{E}_s\rangle$ and the correlation function between fluctuating quantities $\Delta\widetilde{E}_s$ and $\Delta\widetilde{S}$:

$$\frac{\mathrm{Var}(\Delta\widetilde{E}_s)}{\langle\Delta\widetilde{E}_s\rangle^2} \geqslant \frac{1}{\mathrm{Var}(\widetilde{\mathcal{B}})}\left[\beta_r\frac{\mathrm{Var}(\Delta\widetilde{E}_s)}{\langle\Delta\widetilde{E}_s\rangle} - \frac{\mathrm{Cor}(\Delta\widetilde{E}_s, \Delta\widetilde{S})}{\langle\Delta\widetilde{E}_s\rangle}\right]^2. \tag{12}$$

Equation (12) states that a smaller $\mathrm{Var}(\Delta\widetilde{E}_s)/\langle\Delta\widetilde{E}_s\rangle^2$ requires a smaller difference in the bracket on the right-hand side of Eq. (12) or a larger $\mathrm{Var}(\widetilde{\mathcal{B}})$. We note that a higher precision directly implies a smaller Fano factor, therefore a small difference could occur when the correlation function between energy and information content changes also becomes small, implying a disentanglement between energy and information. Meanwhile, a larger $\mathrm{Var}(\widetilde{\mathcal{B}})$ reflects a worse energetic stability to complete an information processing process. Hence, the above inequality reveals a trade-off relation between precision and the degree of energy-information connection: A more precise energy change inference requires a looser energy-information link.

Compared with the form of thermodynamic uncertainty relation [98–100] which lower bounds the precision using the averaged total entropy production, the lower bound on precision obtained herein depends on the fluctuating system's von Neumann entropy production. Without referring to the total entropy production, which can become ill-defined in scenarios involving nonthermal and unknown environments [89], we expect Eq. (12) to hold in generic quantum setups, in direct contrast to the thermodynamic uncertainty relation which can be violated in certain quantum systems [101,102]. The involved correlation function $\mathrm{Cor}(\Delta\widetilde{E}_s, \Delta\widetilde{S})$ in Eq. (12) further reveals how the energetics and information interact at the level of higher-order fluctuations.

We highlight that Eq. (12) is obtained by explicitly treating the fluctuating energetic and information-theoretic quantities on equal footing. Supposing one just considers the mean of the fluctuating system's information content change by neglecting its fluctuations, one readily finds that $\widetilde{\mathcal{E}} - \langle\widetilde{\mathcal{E}}\rangle \to \Delta\widetilde{E}_s - \langle\Delta\widetilde{E}_s\rangle$ and the correlation function $\mathrm{Cor}(\Delta\widetilde{E}_s, \Delta\widetilde{S})$ vanishes. Under this special circumstance, Eq. (12) reduces to a trivial equality which relates the precision to the Fano factor, $\mathrm{Var}(\Delta\widetilde{E}_s)/\langle\Delta\widetilde{E}_s\rangle^2 = [\mathrm{Var}(\Delta\widetilde{E}_s)/\langle\Delta\widetilde{E}_s\rangle]^2/\mathrm{Var}(\Delta\widetilde{E}_s)$. By including the fluctuations of system's information content change, Eq. (12) immediately becomes a nontrivial inequality between the precision and the Fano factor due to the presence of a nonzero correlation function.

By replacing $\Delta\widetilde{E}_s$ with $\Delta\widetilde{S}$ in Eq. (11), we can establish a universal lower bound on the precision $\mathrm{Var}(\Delta\widetilde{S})/\langle\Delta\widetilde{S}\rangle^2$ of the fluctuating system's information content change $\Delta\widetilde{S}$ as well:

$$\frac{\mathrm{Var}(\Delta\widetilde{S})}{\langle\Delta\widetilde{S}\rangle^2} \geqslant \frac{1}{\mathrm{Var}(\widetilde{\mathcal{B}})}\left[\frac{\mathrm{Var}(\Delta\widetilde{S})}{\langle\Delta\widetilde{S}\rangle} - \beta_r\frac{\mathrm{Cor}(\Delta\widetilde{E}_s, \Delta\widetilde{S})}{\langle\Delta\widetilde{S}\rangle}\right]^2. \tag{13}$$

The form of Eq. (13) bears a close resemblance to that of Eq. (12) with a common contribution from the correlation function $\mathrm{Cor}(\Delta\widetilde{E}_s, \Delta\widetilde{S})$. Similarly, Eq. (13) implies that a more precise inference of information content change requires a looser energy-information link. Our results Eqs. (12) and (13) together thus indicate that higher-order fluctuations of the system's energy and information content changes should also be linked, highlighting the necessity of under-

standing the connection between energetics and information from the trajectory level.

Before proceeding, we summarize that the general bounds on averaged thermodynamic quantities [cf. Eq. (8)] and precision [cf. Eqs. (12) and (13)] are obtained as direct results of the non-negativity of the quantum relative entropy and the Cauchy-Schwarz inequality, respectively. These are rather general mathematical properties holding regardless of the details of the system and the environment. Hence, the general links obtained in this section should inherit such a generality as well as mathematical soundness.

## IV. NUMERICAL DEMONSTRATIONS

In this section, we present a set of numerical demonstrations to illustrate the performance of the obtained general links in detailed systems. We select models that first enable us to obtain numerical results for the involved energetic and information-theoretical quantities such that we can have benchmarks to evaluate the performance of the thermodynamic bounds and, second, cover a diversity of environments such that we can also demonstrate the generality of the thermodynamic framework. We remark that detailed models may invoke certain assumptions about their system Hamiltonian, environments, and dissipative evolution to define their contexts, but our general links hold irrespective of such details and are applicable far more broadly.

### A. Single thermal environment: Quantum information erasure

We first investigate the isothermal scenario with a single thermal bath of temperature $T_E$ where the majority of studies on thermodynamics of information were conducted. For concreteness, we consider a driven qubit immersed in a single thermal bath which was used to realize an information erasure process [35,36], as Fig. 2(a) sketches. The driven qubit is described by a time-dependent Hamiltonian:

$$H_s(t) = \frac{\varepsilon(t)}{2}(\cos[\theta(t)]\sigma_z + \sin[\theta(t)]\sigma_x). \tag{14}$$

Here, $\sigma_{x,z}$ denote the Pauli matrices, and we have two driving fields $\varepsilon(t)$ and $\theta(t)$. We adopt the driving protocols $\varepsilon(t) = \varepsilon_0 + (\varepsilon_\tau - \varepsilon_0)\sin(\pi t/2\tau)^2$ and $\theta(t) = \pi(t/\tau - 1)$ [36], with $\tau$ being the time duration of the information erasure process. Setting $\varepsilon_\tau \gg \varepsilon_0$ and $\varepsilon_\tau/T_E \gg 1$, one can reset the qubit to a final state that is very close to its ground state, thus realizing an information erasure process.

The evolution of the actual system state $\rho_s(t)$ is governed by a quantum Lindblad master equation [35]:

$$\frac{d}{dt}\rho_s(t) = -i[H_s(t), \rho_s(t)] + \sum_{\mu=1}^{2}\gamma_\mu \mathcal{D}[L_\mu(t)]\rho_s(t). \tag{15}$$

Here, $\gamma_\mu \geqslant 0$ is the damping coefficient of decaying channel $\mu$, $\mathcal{D}[L_\mu]\rho = L_\mu\rho L_\mu^\dagger - \frac{1}{2}\{L_\mu^\dagger L_\mu, \rho\}$ denotes a Lindblad superoperator with $\{\mathcal{O}_1, \mathcal{O}_2\} = \mathcal{O}_1\mathcal{O}_2 + \mathcal{O}_2\mathcal{O}_1$. We have two time-dependent jump operators $L_1(t) = \sqrt{\varepsilon(t)[N_E(t)+1]}|0_t\rangle\langle 1_t|$, $L_2(t) = \sqrt{\varepsilon(t)N_E(t)}|1_t\rangle\langle 0_t|$ describing de-excitation and excitation process induced by the thermal bath, respectively. Here $|0_t\rangle$ ($|1_t\rangle$) is the instantaneous ground (excited) state of $H_s(t)$, $N_E(t) = 1/[e^{\varepsilon(t)/T_E} - 1]$ is the Bose-Einstein distribution.

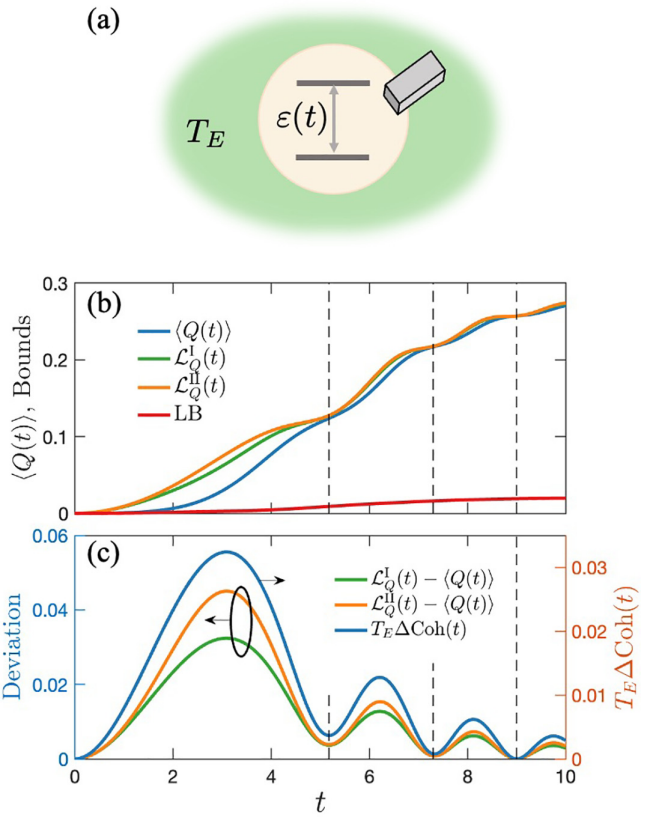


FIG. 2. (a) Sketch of a driven qubit coupled to a single thermal bath with temperature $T_E$. (b) We present the averaged heat dissipation $\langle Q(t)\rangle$ (blue line) and contrast upper bounds $\mathcal{L}_Q^{\rm I,II}(t)$ (green and orange lines, respectively) from the two thermodynamic inference schemes against the Landauer bound (LB) '$-T_E\langle\Delta\widetilde{S}(t)\rangle$' (red line). (c) We depict the deviations $\mathcal{L}_Q^{\rm I,II}(t) - \langle Q(t)\rangle$ (left axis) and quantum coherence generation $T_E\Delta{\rm Coh}(t)$ (right axis, see definition in the main text) as a function of time. Parameters are $\gamma_{1,2} = 0.2$, $T_0 = T_E = 1/8$, $\varepsilon_0 = 0.4$, $\varepsilon_\tau = 4$, and $\tau = 10$.

Together with Eqs. (14) and (15), one can then obtain numerical results for $\langle Q(t)\rangle$ and $\langle W(t)\rangle$ based on their definitions given above Eq. (8). To numerically evaluate the upper bounds $\mathcal{L}_Q^{\rm I,II}(t)$ in Eq. (9), one just takes the simulated $\rho_s(t)$ from Eq. (15) and $H_s(t)$ as the inputs for the two thermodynamic inference schemes and Eq. (9). Even though Eq. (15) depends on $T_E$ explicitly, which is one of defining features of the current model, it is worth clarifying that the upper bounds $\mathcal{L}_Q^{\rm I,II}(t)$ remain agnostic about the environment, as one cannot tell whether the environment is of a thermal nature based solely on numerical results for $\rho_s(t)$ and $H_s(t)$. Particularly, it is often the case that $\rho_s(t)$ is a nonequilibrium state due to finite-time driving.

Without loss of generality, we consider a driven qubit initially at the thermal equilibrium with the bath and set the parameter $T_0 = T_E$. We point out that such a choice does not compromise the generality of the upper bounds in Eq. (9). We first focus on the behavior of the actual heat dissipation $\langle Q(t)\rangle$ and contrast upper bounds $\mathcal{L}_Q^{\rm I,II}(t)$ obtained herein against the Landauer bound $-T_E\langle\Delta\widetilde{S}(t)\rangle$ since we work in the weak coupling limit as indicated by the quantum Lindblad

equation Eq. (15). We depict a typical set of numerical results in Fig. 2(b). From Fig. 2(b), we clearly observe that the actual heat dissipation $\langle Q(t)\rangle$ is well above the Landauer bound at finite times as expected. In comparison, the upper bounds $\mathcal{L}_Q^{\mathrm{I,II}}(t)$ provide much tighter descriptions due to the inclusion of extra state-dependent and process-dependent contributions, as pointed out in the previous section. Moreover, we see that the upper bounds $\mathcal{L}_Q^{\mathrm{I,II}}(t)$ are capable of capturing the fine oscillating behavior of the actual heat dissipation $\langle Q(t)\rangle$, unlike the Landauer bound.

Contrasting the performance of the two upper bounds $\mathcal{L}_Q^{\mathrm{I,II}}(t)$, we depict the deviations $\mathcal{L}_Q^{\mathrm{I,II}}(t) - \langle Q(t)\rangle$ (left axis) in Fig. 2(c). We find that the upper bound $\mathcal{L}_Q^{\mathrm{I}}(t)$ outperforms its counterpart $\mathcal{L}_Q^{\mathrm{II}}(t)$, especially at short times. Recalling that $\mathcal{L}_Q^{\mathrm{I}}(t)$ is evaluated using $\rho_r^{\mathrm{I}}(t)$ that is obtained from the equal-energy inference scheme, we attribute its relative better performance to the fact that the internal energy of the system represents a better estimator than the information content of the system for inferring the parameter $\beta_r(t)$, after all $H_s(t)$ and $\beta_r(t)$ represent a conjugate pair in a Gibbsian state.

To pinpoint the origin of oscillating behaviors of the deviations $\mathcal{L}_Q^{\mathrm{I,II}}(t) - \langle Q(t)\rangle$ as a function of time, we turn to the quantum coherence generated during the process which is preserved in our framework. We adopt the quantum coherence measure proposed by Ref. [103], $\mathrm{Coh}(t) \equiv S'(t) - S(t)$, with $S'(t) = -\mathrm{Tr}(\Pi[\rho_s(t)]\ln\Pi[\rho_s(t)])$ denoting the von Neumann entropy of a diagonal state $\Pi[\rho_s(t)] = \sum_n |E_n(t)\rangle\langle E_n(t)|\rho_s(t)|E_n(t)\rangle\langle E_n(t)|$ in the instantaneous energy basis $\{|E_n(t)\rangle\}$ of $H_s(t)$. Recent studies [104,105] have highlighted the vital role of quantum coherence in shaping the energetics of the system by adopting this measure. In Fig. 2(c), we also depict the result of quantum coherence generation $\Delta\mathrm{Coh}(t) \equiv \mathrm{Coh}(t) - \mathrm{Coh}(0)$ during the process (right axis). We clearly observe that the deviations follow perfectly with the oscillating quantum coherence generation, providing strong evidence that quantum coherence is responsible for the variations of the deviations $\mathcal{L}_Q^{\mathrm{I,II}}(t) - \langle Q(t)\rangle$. The matched local minima of the deviations and the quantum coherence generation suggest that one can obtain tighter upper bounds by suppressing the quantum coherence. We verify this strategy numerically in Appendix B. Given the nontrivial role of the quantum coherence in energetics, it is thus essential for a thermodynamic framework concerning relations between energetics and information to preserve quantum coherence generated during the process.

Interestingly, we find that the driven qubit can perform work with $\langle W(t)\rangle > 0$, providing a test bed for contrasting upper bounds on the extracted work $\langle W(t)\rangle$. In this model, we have checked that the work extraction process accompanies a continuous reduction in the system's information content $\langle\Delta\widetilde{S}(t)\rangle$. Thus, the driven qubit functions in a way similar to a noncyclic information engine which, by definition, operates with a single thermal bath and utilizes system's information as a resource [96]. We stress that there is no contradiction with the second law of thermodynamics as we have checked that the total entropy production $\langle\Delta\widetilde{S}(t)\rangle + \langle Q(t)\rangle/T_E$ remains non-negative during the information erasure process. As the quantum Lindblad master equation can be recast as the result of continuous measurements by the environment [106],

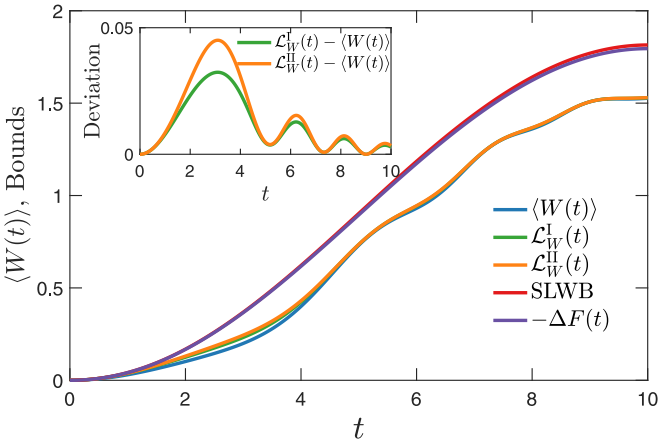


FIG. 3. Averaged extracted work $\langle W(t)\rangle$ (blue line) from a driven qubit. We contrast upper bounds $\mathcal{L}_W^{\mathrm{I,II}}(t)$ (green and orange lines, respectively) from the two thermodynamic inference schemes against a form of the second-law work bound (SLWB) $-\Delta F(t) - T_E\langle\Delta\widetilde{S}(t)\rangle$ (red line, see elaboration in the main text) and the free energy bound $-\Delta F(t)$ (purple line). In the inset, we depict the deviations $\mathcal{L}_W^{\mathrm{I,II}} - \langle W(t)\rangle$. Parameters are the same as Fig. 2.

we adopt a form of the second-law work bound $-\Delta F(t) - T_E\langle\Delta\widetilde{S}(t)\rangle$ generalized to account for continuous measurements [95] for comparison.

In Fig. 3, we depict numerical results for the extracted work $\langle W(t)\rangle$ and contrast our upper bounds $\mathcal{L}_W^{\mathrm{I,II}}(t)$ against the second-law work bound $-\Delta F(t) - T_E\langle\Delta\widetilde{S}(t)\rangle$ and the free energy bound $-\Delta F(t)$. The predictions of the latter two are almost indistinguishable in this scenario. From Fig. 3, it is evident that the two upper bounds $\mathcal{L}_W^{\mathrm{I,II}}(t)$ obtained herein outperform the second-law work bound and the free energy bound not only by their tightness, as highlighted by the magnitudes of deviations $\mathcal{L}_W^{\mathrm{I,II}} - \langle W(t)\rangle$ shown in the inset of Fig. 3, but also with an ability to capture the fine oscillating behavior of $\langle W(t)\rangle$ at finite times induced by quantum coherence (see results in Fig. 2). We attribute the latter capability to the fact that $\mathcal{L}_W^{\mathrm{I,II}}(t)$ include contributions which are process dependent, unlike the second-law work bound and the free-energy bound which only take into account state function changes. We thus envision that the two upper bounds $\mathcal{L}_W^{\mathrm{I,II}}(t)$ can provide tighter finite-time constraints than their counterparts derived from the second law of thermodynamics. In the limit of quasistatic driving, we note that the two bounds $\mathcal{L}_W^{\mathrm{I,II}}(t)$ reduce to the free-energy bound $-\Delta F(t)$ as a result of Landauer's principle $\langle Q(t)\rangle = -T_E\langle\Delta\widetilde{S}(t)\rangle$ achieved in that limit and the fact that the system always stays in an instantaneous thermal equilibrium state.

### B. Multiple thermal environments: Inelastic heat transfer

We next turn to a scenario involving multiple thermal baths where the existing bounds relying on a single bath temperature such as the Landauer bound become inapplicable. In the presence of multiple thermal baths, we remark that the averaged heat dissipation $\langle Q(t)\rangle$ considered here corresponds to the net sum of heat components flowing into each bath, according to the first law of thermodynamics. One is unable

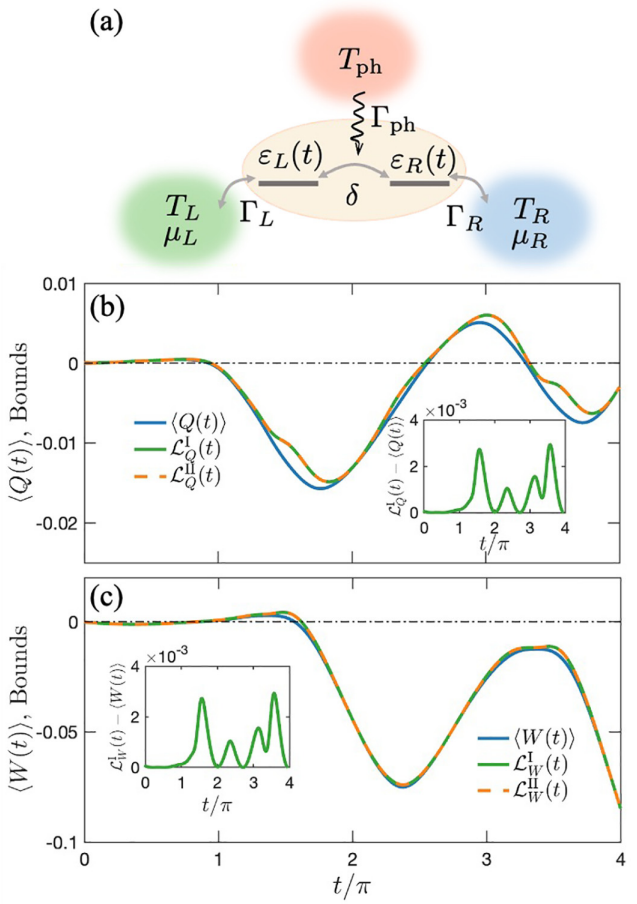


FIG. 4. (a) Sketch of a three-terminal double quantum dot setup in which a driven double quantum dot system tunnel-couples to two electronic baths whose internal hopping is further affected by a phononic bath. (b) The averaged heat dissipation $\langle Q(t)\rangle$ (blue line) and upper bounds $\mathcal{L}_Q^{\rm I,II}(t)$ (green solid and orange dashed lines, respectively) from the two thermodynamic inference schemes. Inset: The deviation $\mathcal{L}_Q^{\rm I}(t) - \langle Q(t)\rangle$. (c) The averaged extracted work $\langle W(t)\rangle$ (blue line) and upper bounds $\mathcal{L}_W^{\rm I,II}(t)$ (green solid and orange dashed lines, respectively) from the two thermodynamic inference schemes. Inset: The deviation $\mathcal{L}_W^{\rm I}(t) - \langle W(t)\rangle$. Parameters are $\mu_L = \mu_R = 0$, $\Omega = 1$, $\varepsilon_{L0} = 2$, $\varepsilon_{R0} = 2$, $\varepsilon_{L\tau} = 1.5$, $\varepsilon_{R\tau} = 1.5$, $\phi = \pi/4$, $\Gamma_L = \Gamma_R = \Gamma_{\rm ph} = 0.1$, $\delta = 0.2$, $T_L = 0.2$, $T_R = 0.3$, $T_{\rm ph} = 0.4$ and the initial system Gibbsian state is fixed by setting $T_0 = 0.25$.

to decompose $\langle Q(t)\rangle$ to get an individual heat component for each bath given the knowledge of the system only. In contrast, the work definition adopted here still quantifies the amount of extractable work from the total setup, regardless of the number of baths, provided that only the system is being driven.

To examine the performance of both upper bounds $\mathcal{L}_{Q,W}(t)$, we specifically consider a driven three-terminal system [107,108] that is within the current experimental capabilities. The total setup consists of a double quantum dot system (specified as the $L$ and $R$ dots) coupled to a phononic thermal bath, while each dot further individually exchanges electrons with an electronic thermal reservoir, as Fig. 4(a) depicts. The total Hamiltonian for the setup contains three different parts. The first part of the total Hamiltonian describes the "bare" system–two coupled quantum dots whose site energies can be tuned:

$$H_{\rm DQD}(t) = \sum_{i=L,R} \varepsilon_i(t) d_i^\dagger d_i + \delta(d_L^\dagger d_R + {\rm H.c.}). \tag{16}$$

Here, H.c. denotes the Hermitian conjugate of the term in the bracket, $d_i$ and $\varepsilon_i(t)$ denote an electronic annihilation operator and a time-dependent site energy of the $i$th quantum dot, respectively. We adopt the driving protocols $\varepsilon_L(t) = \varepsilon_{L0} + \varepsilon_{L\tau}\sin(\Omega t)$, $\varepsilon_R(t) = \varepsilon_{R0} + \varepsilon_{R\tau}\sin(\Omega t + \phi)$, with $\Omega$ and $\phi$ being the frequency and the nonzero modulation phase, respectively [109,110]. This simple set of driving protocols is sufficient for demonstration purposes. $\delta$ measures the tunneling strength between the two dots.

The second part of the total Hamiltonian accounts for a phononic thermal bath containing an ensemble of harmonic oscillators and their inelastic coupling to the two dots. The $q$th harmonic oscillator has frequency $\omega_q$ with annihilation operator $a_q$ and $q$-dependent electron-phonon coupling strength $\lambda_q$, resulting in a Hamiltonian denoting the second part $H_{ep} = \sum_q[\omega_q a_q^\dagger a_q/2 + \lambda_q d_L^\dagger d_R(a_q + a_q^\dagger) + {\rm H.c.}]$ [111,112]. The third part of the total Hamiltonian describes two electronic reservoirs with electronic annihilation operators $\{d_{vk}\}$ and energies $\{\varepsilon_{vk}\}$ as well as their coupling to the individual dot measured by a mode-dependent coupling strength $\{\gamma_{vk}\}$, leading to a Hamiltonian describing the third part, $H_{e-{\rm lead}} = \sum_{v=L,R}\sum_k(\varepsilon_{vk} d_{vk}^\dagger d_{vk}/2 + \gamma_{vk} d_v^\dagger d_{vk} + {\rm H.c.})$. The influence of phononic and electronic baths is captured by the spectral functions (or hybridization energies) $\Gamma_{\rm ph} = 2\pi\sum_q \lambda_q^2\delta(\omega - \omega_q)$ and $\Gamma_v = 2\pi\sum_k |\gamma_{vk}|^2\delta(\varepsilon - \varepsilon_{vk})$ ($v = L, R$), respectively. For simplicity, they are chosen to be flat (wide-band limit).

We consider the weak coupling limit in which both the electron-phonon and dot-reservoir couplings can be treated in a perturbative manner. Denoting $V = \sum_q \lambda_q d_L^\dagger d_R(a_q + a_q^\dagger) + \sum_{v=L,R}\sum_k \gamma_{vk} d_v^\dagger d_{vk} + {\rm H.c.}$ as the overall coupling Hamiltonian, the evolution dynamics of the reduced system state $\rho_s$ is then governed by the following Redfield master equation [16]:

$$\frac{\partial}{\partial t}\rho_s(t) = i[\rho_s(t), H_{\rm DQD}(t)] - \int_0^\infty d\tau {\rm Tr}_E\{[V, [V(-\tau), \rho_s(t)\rho_E]]\}. \tag{17}$$

Here, $\rho_s(t)\rho_E$ is short for $\rho_s(t)\otimes\rho_E$, $\rho_E = \rho_L\otimes\rho_R\otimes\rho_{\rm ph}$ denotes an initial product thermal state for the phononic and electronic baths where $\rho_{\rm ph} = \exp[-\beta_{\rm ph}H_{\rm ph}]/{\rm Tr}\{\exp[-\beta_{\rm ph}H_{\rm ph}]\}$ and $\rho_v = \exp[-\beta_v(H_v - \mu_v N_v)]/{\rm Tr}\{\exp[-\beta_v(H_v - \mu_v N_v)]\}$ ($v = L, R$), with $H_{\rm ph} = \sum_q \omega_q a_q^\dagger a_q$, $H_v = \sum_k \varepsilon_{vk} d_{vk}^\dagger d_{vk}$, and $N_v = \sum_k d_{vk}^\dagger d_{vk}$. $\beta_{\rm ph} = T_{\rm ph}^{-1}$ and $\beta_v = T_v^{-1}$ denote inverse bath temperatures. $\mu_v$ are chemical potentials of the electronic reservoirs. Numerical values for $\langle Q(t)\rangle$ and $\langle W(t)\rangle$ can be obtained by evolving Eq. (17) after specifying parameter values.

The setup can function as an inelastic heat engine by setting the electronic bath temperatures to be equal, $T_L = T_R$ [110]. Here we are interested in demonstrating the utility of Eq. (8) in a scenario with multiple thermal baths of different temperatures, so we just take an arbitrary set of parameters with $T_L \neq T_R \neq T_{\rm ph}$, in particular. To avoid misinterpretations on our framework, we should clarify the role of bath temperatures

in the simulation: To get numerical results for $\langle Q(t)\rangle$ and $\langle W(t)\rangle$, we need values for bath temperatures as the initial condition to evolve Eq. (17), similar in spirit to the first model simulated in Sec. IV A. However, the evaluations of the upper bounds in Eq. (8) just require $\rho_s(t)$ and $H_s(t)$ as inputs, and the former can be even extracted using techniques such as the quantum state tomography without actually knowing the underlying equation of motion. Hence, our statement that our framework requires just the knowledge of the system remains valid even though we select a specific model which requires bath temperatures to define the context. To highlight that upper bounds stay regardless of bath temperatures, we further set $T_0 \neq T_i$ $(i = L, R, \text{ph})$ in Eq. (9).

We depict a set of numerical results in Fig. 4 by numerically solving Eq. (17) in the nonlocal energy basis. From Figs. 4(b) and 4(c) and insets therein, we clearly observe the expected features of $\mathcal{L}_Q^{\mathrm{I,II}}(t)$ and $\mathcal{L}_W^{\mathrm{I,II}}(t)$ as being upper bounds on $\langle Q(t)\rangle$ and $\langle W(t)\rangle$, respectively. Particularly, both upper bounds $\mathcal{L}_Q^{\mathrm{I,II}}(t)$ capture well the oscillating behavior and magnitude of $\langle Q(t)\rangle$ regardless of its sign changes during the process, and similar performance holds for upper bounds $\mathcal{L}_W^{\mathrm{I,II}}(t)$ on $\langle W(t)\rangle$. We have checked that the two upper bounds $\mathcal{L}_Q^{\mathrm{I,II}}(t)$ are almost identical with a difference of the order of $10^{-5}$ under the chose parameter set, the same for $\mathcal{L}_W^{\mathrm{I,II}}(t)$. From the figure, we also notice that the setup depicts rich functional behaviors over the course of the evolution. Notably, during the time interval $3 \lesssim t \lesssim 4.9$, the setup can function as a heat engine performing work while absorbing a net amount of heat from baths ($\langle Q(t)\rangle < 0$ and $\langle W(t)\rangle > 0$). The setup can also function as a heat dissipator consuming external work ($\langle Q(t)\rangle > 0$ and $\langle W(t)\rangle < 0$) or an energy sink absorbing both heat and work ($\langle Q(t)\rangle < 0$ and $\langle W(t)\rangle < 0$). However, identifying their individual operational regimes in the parameter space is beyond the scope of this paper.

### C. Dissipation-engineered environment: Dissipative quantum state preparation

To further highlight the generality of our framework, we now consider an extreme scenario in which introducing the notion of temperature becomes completely in vain. A notable example of this scenario concerns dissipation-engineered quantum processes where one can harness environmental dissipation, which is usually thought to be detrimental as a useful resource for quantum tasks through dissipation engineering. Dissipation-engineered quantum processes have already found a wide range of applications in quantum information processing (see a recent review [66] and references therein). For dissipation-engineered quantum processes, one has no knowledge about the environment associated with the engineered dissipation and thus cannot make *a priori* assumptions about the nature of the environment, rendering existing thermodynamic bounds which require environmental information (for instance, temperature) to hold inapplicable. In comparison, the details of the engineered dynamical evolution of the system could be available [66]. Hence the dissipation-engineered quantum process provides an intriguing platform for illustrating the generality of our framework.

To provide a concrete demonstration, we investigate the so-called dissipative quantum state preparation process in which

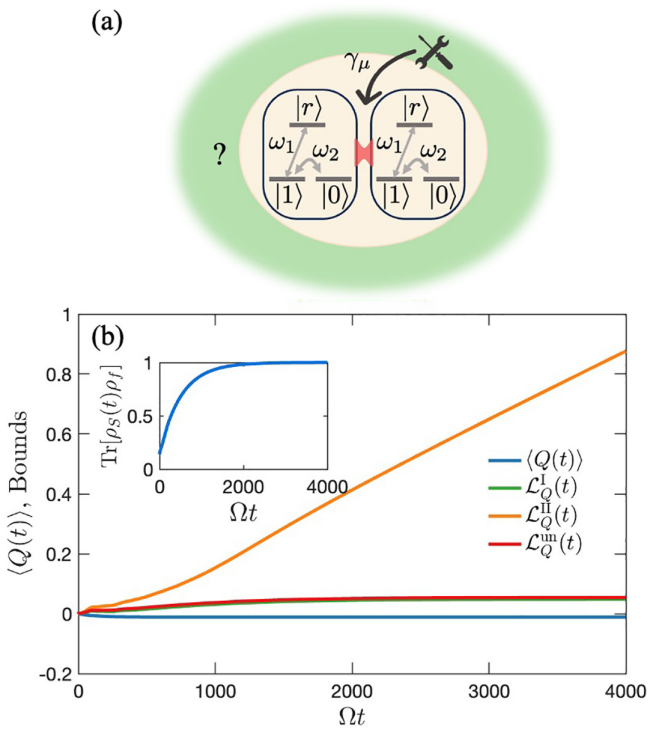


FIG. 5. (a) Sketch of a double Rydberg atom system, each consisting of two ground states $|0, 1\rangle$ and one Rydberg state $|r\rangle$, used to prepare an entangled Bell state through engineered dissipation whose associated environment remains unknown. (b) Heat dissipation $\langle Q(t)\rangle$ (blue line) during a dissipative quantum Bell state preparation process. We contrast the obtained upper bounds $\mathcal{L}_Q^{\mathrm{I,II}}(t)$ (green and orange lines, respectively) from the two thermodynamic inference schemes and a simplified one $\mathcal{L}_Q^{\mathrm{un}}(t)$ (red line) valid for undriven systems. Inset: Fidelity $\mathrm{Tr}[\rho_s(t)\rho_f]$ as a function of time. We adopt the experimental parameters $(\omega_1, \omega_2, \gamma_\mu) = 2\pi \times (0.02, 0.01, 0.015)$ MHz [113], choose $\beta_0 = 30$ to fix the initial Gibbsian state of the system, and set $\Omega = 2\pi$ MHz as the unit.

one prepares desired pure quantum states at steady states of engineered dissipative evolution processes [114–117]. This quantum state preparation process has been realized experimentally [61,62,67,118–121]. We choose a double Rydberg atom system designed to prepare the Bell state [122] in a dissipative manner, as Fig. 5(a) shows. The model consists of two $\Lambda$-type three-level Rydberg atoms—each one contains two ground states $|0\rangle$ and $|1\rangle$, and one Rydberg state $|r\rangle$. Under an unconventional Rydberg pumping mechanism, the effective Hamiltonian of the coupled Rydberg atom system reads [122]

$$H_s = \omega_1(|10\rangle\langle r0| + |01\rangle\langle 0r|) + \omega_2[(|11\rangle + |00\rangle) \otimes (\langle 01| + \langle 10|)] + \mathrm{H.c.} \quad (18)$$

Here, a two-atom state $|ab\rangle$ is understood as $|a\rangle \otimes |b\rangle$ with $a, b = 0, 1, r$. The engineered evolution of the system is governed by a quantum master equation of the Lindblad form as Eq. (15) shows, with the Hamiltonian given by Eq. (18) and four Lindblad jump operators describing engineered spontaneous emission in the two-atom state basis [122]: $L_1 = |01\rangle\langle 0r|$, $L_2 = |00\rangle\langle 0r|$, $L_3 = |10\rangle\langle r0|$ and $L_4 = |00\rangle\langle r0|$.

Given the Hamiltonian and Lindblad jump operators, one can check that the Bell state $|\Phi\rangle = (|00\rangle - |11\rangle)/\sqrt{2}$ turns out to be the fixed point of the evolution, $\frac{d}{dt}\rho_f = 0$ with $\rho_f = |\Phi\rangle\langle\Phi|$ due to the properties that $H_S|\Phi\rangle = 0$ and $L_\mu|\Phi\rangle = 0$, $\forall\mu$. These two properties are, in fact, the prerequisite for getting an entangled pure state using dissipative Markovian evolution [115]. As the system stays in a pure state in the long time limit, the total entropy production becomes ill-defined [123], hence one cannot resort to the second law of thermodynamics to connect energetics and information for this process.

As the model is time independent, we only need to focus on the averaged heat dissipation $\langle Q(t)\rangle$ whose numerical values can be obtained by evolving the corresponding quantum Lindblad master equation subject to an initial Gibbsian state. We depict numerical results for $\langle Q(t)\rangle$ as well as predictions from the obtained upper bounds $\mathcal{L}_Q^{\mathrm{I,II}}(t)$ [cf. Eq. (9)] and $\mathcal{L}_Q^{\mathrm{un}}(t)$ [cf. Eq. (10)] in Fig. 5. From Fig. 5(b), we observe that all derived upper bounds herein are valid, constraining the heat dissipation from the above. Among them, we find that the bound $\mathcal{L}_Q^{\mathrm{I}}(t)$ with $\beta_r(t)$ evaluated using the equal-energy inference scheme stands out as the tightest, whereas the bound $\mathcal{L}_Q^{\mathrm{II}}(t)$ with $\beta_r(t)$ evaluated using the equal-information-content inference scheme defines the worst scenario, with a prediction significantly deviating from the actual heat dissipation. We attribute this large deviation to the fact that the inferred value of $\beta_r(t)$ tends to be large when applying the equal-information-content inference scheme to a system in a pure state.

From Fig. 5(b), we also note that the simplified bound $\mathcal{L}_Q^{\mathrm{un}}(t)$ works well with a prediction slightly larger than that of the best $\mathcal{L}_Q^{\mathrm{I}}(t)$. Hence, to implement the equal-information-content inference scheme for this undriven system, one could instead consider a time-independent reference state, since implementing the equal-information-content inference scheme at the initial time can yield a finite $\beta_r$, which just equals $\beta_0$. We further find that the bounds $\mathcal{L}_Q^{\mathrm{I}}(t)$ and $\mathcal{L}_Q^{\mathrm{un}}(t)$ can capture the saturation behavior of the actual heat dissipation at large times as the system approaches the desired Bell state (see results for the fidelity $\mathcal{F}(t) = \mathrm{Tr}[\rho_s(t)\rho_f]$ shown in the inset), in direct contrast to the worst bound $\mathcal{L}_Q^{\mathrm{II}}(t)$, which keeps increasing.

### D. Verifying lower bound on precision

At last, we illustrate the performance of lower bounds on precision in Eqs. (12) and (13). Given a detailed model, the mean and variance involved in Eqs. (12) and (13) can be evaluated as follows: First, one obtains the full state $\rho_s(t)$ and single trajectories by evolving the initial Gibbsian state $\rho_s(0)$ and energy eigenstates of the initial system Hamiltonian using the specified quantum channel (i.e., a complete positive and trace-preserving dynamical map), respectively. The parameter $\beta_r(t)$ in the Gibbsian reference state can then be inferred using the two thermodynamic inference schemes with inputs $\rho_s(t)$ and $H_s(t)$. Second, one computes the changes $\Delta\widetilde{E}_s(t)$, $\Delta\widetilde{S}(t)$ as well as the excess energy $\mathcal{E}(t)$ for each trajectory using the numerical outcomes of the first step. At last, one calculates the ensemble averages according to the definition $\langle\mathcal{O}\rangle = \sum_{p_0} p_0\mathcal{O}$ over the complete set of initial measurement probabilities $\{p_0\}$ whose number of elements depends on the dimension of the system Hamiltonian.

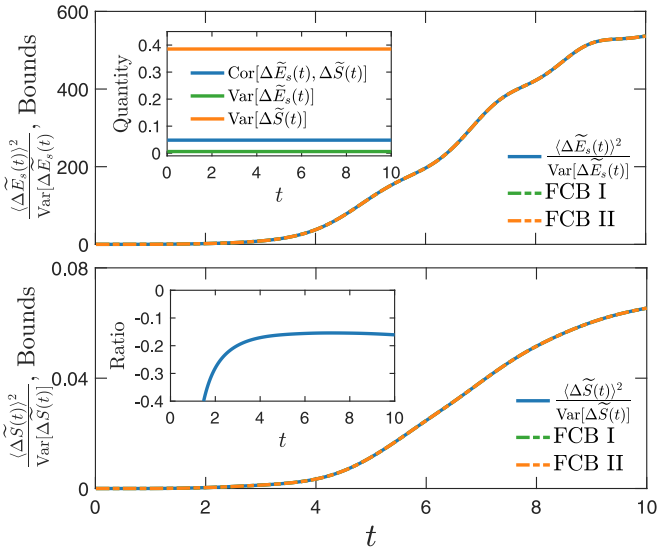


FIG. 6. Inverse of the precision (blue line) of the fluctuating quantities $\Delta\widetilde{E}_s(t)$ (upper panel) and $\Delta\widetilde{S}(t)$ (lower panel) for the model studied in Sec. IV A. We also depict results for the Fano-correlation bounds (FCB) I (green dashed line) and II (orange dashed line) evaluated using the equal-energy and equal-information-content thermodynamic inference scheme, respectively. Upper inset: Correlation function $\mathrm{Cor}(\Delta\widetilde{E}_s, \Delta\widetilde{S})$ (blue line), variance $\mathrm{Var}[\Delta\widetilde{E}_s(t)]$ (green line), and variance $\mathrm{Var}[\Delta\widetilde{S}(t)]$ (orange line). Lower inset: Ratio $[\Delta\widetilde{E}_s(t) - \langle\Delta\widetilde{E}_s(t)\rangle]/[\beta_r(t)\widetilde{\mathcal{E}}(t) - \langle\beta_r(t)\widetilde{\mathcal{E}}(t)\rangle]$. Parameters are the same with Fig. 2.

We adopt the model in Sec. IV A for a detailed illustration. We depict a set of results for $t > 0$ in Fig. 6. To enable a better illustration, we plot the inverse of the precision $\langle\mathcal{O}\rangle^2/\mathrm{Var}(\mathcal{O})$ with $\mathcal{O} = \Delta\widetilde{E}_s, \Delta\widetilde{S}$ and turn the right-hand side of Eqs. (12) and (13) into upper bounds on the inverse of the precision, which we dub Fano-correlation bounds for later convenience. From Fig. 6, we observe that the values of the precision of $\Delta\widetilde{E}_s$ and $\Delta\widetilde{S}$ are rather distinct, with the latter experiencing a relatively larger fluctuation as also manifested by the variance result shown in the inset of Fig. 6(a). This contrast implies that higher-order fluctuation of the system's information content change cannot be neglected in small systems, thereby deserving a faithful treatment. Meanwhile, we notice a nonzero correlation between $\Delta\widetilde{E}_s$ and $\Delta\widetilde{S}$ at finite times as can be seen from the inset of Fig. 6(a). This confirms our expectation that Eqs. (12) and (13) are nontrivial relations linking higher-order fluctuations of energetic and information-theoretic quantities.

We have checked that the Fano-correlation bounds evaluated using the two thermodynamic inference schemes are rather tight in the adopted model with deviations of the order of $10^{-5}$. To understand such a tightness, we numerically calculate the ratio $[\Delta\widetilde{E}_s(t) - \langle\Delta\widetilde{E}_s(t)\rangle]/[\beta_r(t)\widetilde{\mathcal{E}}(t) - \langle\beta_r(t)\widetilde{\mathcal{E}}(t)\rangle]$, with results shown in the inset of Fig. 6(b). From the inset, we find that this ratio remains almost a constant for $t \gtrsim 3$. Therefore, the equality condition of the Cauchy-Schwarz inequality Eq. (11), which requires a strictly constant ratio, is approximately satisfied in the current scenario at large times, explaining the tightness of the two Fano-correlation bounds in the current model. Nevertheless, we remark that one should not expect such a tightness depicted in Fig. 6 to

exist in other models before running numerical simulations, even though the Fano correlation applies a wide range of applications not limited to the current model.

## V. DISCUSSION AND CONCLUSION

We developed a systematic framework to infer links between energetics and information at finite times for a generic open quantum system at the trajectory level, given just the knowledge of the system. Underpinning this framework, we introduced the notion of excess energy to link energetics and information with a meaningful physical interpretation that it quantifies the net energy gain of the system after completing a finite-time trajectory with a change in the system's information content. By analyzing the fluctuation behaviors of the excess energy, we uncovered general relations between changes in energy and information content of the system that apply to a wide range of contexts. Most remarkably, we obtained a single inequality which integrates upper bounds on averaged heat dissipation and extracted work from the system in terms of the change in the averaged system's information content. We contrasted those bounds with existing ones based on the second law of thermodynamics, highlighting their distinct nature and complementary roles. Concerning higher-order fluctuations, we also revealed the intriguing role of the correlation function between the fluctuating system's energy and information content changes in lower bounding their respective precision. We illustrated the utility of derived general relations at finite times through a number of numerical demonstrations.

We envision that our paper propels us closer to an all-encompassing comprehension of the interplay between energetics and information in dynamical open quantum systems interfacing with an expansive array of environment types—extending beyond the realm of solely thermal baths. More crucially, our results clearly demonstrate that it is possible to understand the intricate interplay between the nonequilibrium thermodynamics and information processing in open quantum systems with just the knowledge of the system, in contrast to previous treatments which require both knowledge of the system and environments.

As a final remark, we note that knowing the dynamical information of the system state and Hamiltonian is usually the prerequisite for conducting quantum controls for information tasks [124]. The recent advance in machine learning even enables one to reconstruct the dynamical information from unknown quantum processes [125] and measurements [126] with high precision. From an experimental point of view, the system's dynamical information can be extracted using mature tools such as quantum state and process tomography [127] as well as time-dependent Hamiltonian reconstruction technique [128] to name just a few, without the need to measure complex environments. Therefore, our results, which perform well at finite times, can be readily evaluated experimentally.

Looking forward to future applications, we believe that our framework will strengthen the synergy between quantum thermodynamics and quantum information processing in complex composite systems where only the knowledge of the dynamical system would be accessible. An interesting application that fits in our framework would be quantum annealing, where one just knows a time-dependent system Hamiltonian [129]. Despite the nontrivial role of quantum annealing in solving optimization problems, its energetic aspect remains largely elusive [130]. In the ideal form of quantum annealing, we can apply the current framework to evaluate the work needed to implement the driven unitary process. For quantum annealing experiencing unknown environmental influences, we can further investigate behaviors of heat dissipation due to system-environment coupling to seek control strategies over unwanted environmental effects. Moreover, the finite-time upper bound on heat dissipation represents a tighter estimation for the actual heat dissipation than the Landauer lower bound, thereby providing a suitable reference for optimizing the energetic cost of finite-time quantum processes. We also expect that the finite-time upper bound on extracted work can find a wide range of applications in quantum thermal and information machines and, particularly, enable a tight estimation on their optimal performance when operating with finite-time cycles and/or nonthermal environments.

## ACKNOWLEDGMENTS

J. Liu acknowledges support from the National Natural Science Foundation of China (Grant No. 12205179), the Shanghai Pujiang Program (Grant No. 22PJ1403900), and start-up funding of Shanghai University. J. Lu acknowledges support from the National Natural Science Foundation of China (Grant No. 12305050), the Natural Science Foundation of Jiangsu Higher Education Institutions of China (Grant No. 23KJB140017). J.-H.J. acknowledges support from the National Key R&D Program of China (2022YFA1404400), the National Natural Science Foundation of China (Grant No. 12125504), and the Hundred Talents Program of the Chinese Academy of Sciences.

## APPENDIX A: GIBBSIAN REFERENCE STATES FROM INFERENCE SCHEMES

In this Appendix, we show that a Gibbsian state has minimal energy (information content) among states having the same information content (energy). We first consider the equal-energy inference scheme set by Eq. (3) in the main text. We compare a Gibbsian state $\rho_g(t) = e^{-\beta_r(t)H_s(t)}/Z_r(t)$ with $Z_r(t) = \mathrm{Tr}[e^{-\beta_r(t)H_s(t)}]$ with an arbitrary non-Gibbsian state $\rho(t)$ that has the same energy with $\rho_g(t)$, namely, $\mathrm{Tr}[H_s(t)\rho_g(t)] = \mathrm{Tr}[H_s(t)\rho(t)]$. Their information content contrast reads (time dependence is suppressed for simplicity)

$$\begin{aligned} S(\rho_g) - S(\rho) &= \mathrm{Tr}[\rho \ln \rho] - \mathrm{Tr}[\rho_g \ln \rho_g] \\ &= \mathrm{Tr}[\rho \ln \rho] + \beta_r \mathrm{Tr}[\rho_g H_s] + \ln Z_r \\ &= \mathrm{Tr}[\rho \ln \rho] + \beta_r \mathrm{Tr}[\rho H_s] + \ln Z_r \\ &= \mathrm{Tr}[\rho(\ln \rho - \ln \rho_g)] \geqslant 0. \end{aligned} \tag{A1}$$

In arriving at the third line, we have utilized the equal-energy condition. The above inequality, being a result of the nonnegativity of quantum relative entropy, tells us that a Gibbsian state $\rho_g$ has minimum information content (maximum von Neumann entropy) among all states having the same energy.

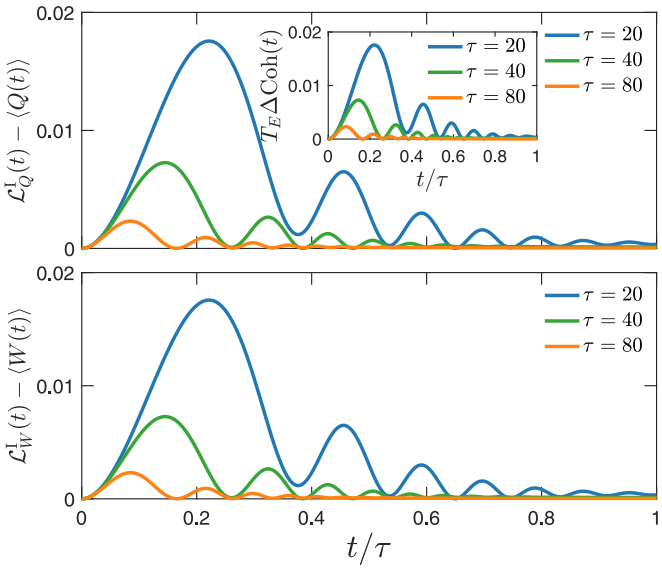


FIG. 7. Upper panel: The deviation $\mathcal{L}_Q^{\rm I}(t) - \langle Q(t)\rangle$ with varying $\tau$. Inset: The quantum coherence generation $T_E\Delta{\rm Coh}(t)$ with varying $\tau$. Lower panel: The deviation $\mathcal{L}_W^{\rm I}(t) - \langle W(t)\rangle$ with varying $\tau$. Parameters are $\gamma_{1,2} = 0.2$, $T_0 = T_E = 1/8$, $\varepsilon_0 = 0.4$, $\varepsilon_\tau = 4$.

Hence, we can set

$$\rho_r^{\rm I}(t) = e^{-\beta_r(t)H_s(t)}/Z_r(t), \tag{A2}$$

with $\beta_r(t)$ determined by ${\rm Tr}[H_s(t)\rho_r^{\rm I}(t)] = \overline{E}_s(t)$ in Eq. (3).

We then turn to the equal-information-content inference scheme governed by Eq. (4). In this case, we compare the Gibbs state $\rho_g(t) = e^{-\beta_r(t)H_s(t)}/Z_r(t)$ with an arbitrary non-Gibbsian state $\rho(t)$ that has the same information content, namely, $S(\rho_g) = S(\rho)$. Their energy contrast reads (time-dependence is suppressed for simplicity)

$$\begin{aligned} E(\rho_g) - E(\rho) &= {\rm Tr}[H_s\rho_g] - {\rm Tr}[H_s\rho] \\ &= -\beta_r^{-1}{\rm Tr}[\rho_g \ln \rho_g] + \beta_r^{-1}{\rm Tr}[\rho \ln \rho_g] \\ &= -\beta_r^{-1}({\rm Tr}[\rho(\ln\rho - \ln\rho_g)]) \leqslant 0. \end{aligned} \tag{A3}$$

In arriving at the third line, we have utilized the equal-information-content condition. To get the inequality, we have noted that $\beta_r$ is generally positive under the equal-information-content condition [88]. Hence, we can infer from the above inequality that a Gibbs state $\rho_g(t)$ has minimum energy among all states having the same information content. We then set

$$\rho_r^{\rm II}(t) = e^{-\beta_r(t)H_s(t)}/Z_r(t), \tag{A4}$$

with $\beta_r(t)$ fixed by $S(\rho_r^{\rm II}(t)) = S(t)$ in Eq. (4).

## APPENDIX B: TUNING THE PERFORMANCE OF UPPER BOUNDS IN AN INFORMATION ERASURE PROCESS

In this Appendix, we explore the strategy of suppressing the quantum coherence to improve the tightness of upper bounds on averaged heat dissipation and extracted work for a quantum information erasure model studied in Sec. IV A. In this model, we note that finite time driving fields will drive the system away from its instantaneous thermal state which is the fixed point of the quantum Lindblad master equation Eq. (15), generating nonzero quantum coherence in the instantaneous energy basis.

As slower driving fields would allow the system state to be closer to the instantaneous thermal state, we hence focus on increasing the time duration $\tau$ of the information erasure process to suppress the quantum coherence. In Fig. 7, we depict a set of results for $\mathcal{L}_Q^{\rm I}(t) - \langle Q(t)\rangle$ and $\mathcal{L}_W^{\rm I}(t) - \langle W(t)\rangle$ with varying $\tau$ as well as the dynamics of the quantum coherence generation shown in the inset. From the figure, it is evident that suppressing the quantum coherence indeed leads to an improvement in the tightness of upper bounds $\mathcal{L}_{Q,W}^{\rm I}(t)$. More generally, we can understand this improvement from the derivation of Eq. (7) in the main text. To get Eq. (7), we have utilized the relation $D[\rho_s(t)||\rho_r(t)] \geqslant 0$ with the equality taken only when $\rho_s(t) = \rho_r(t)$. Hence, as $\rho_s(t)$ gradually approaches a Gibbsian state $\rho_r(t)$ with zero quantum coherence, Eq. (7) tends to become an equality, yielding tighter and tighter upper bounds. Nevertheless, we point out that one cannot completely destroy quantum coherence in such finite time processes. Especially, maintaining a nonzero quantum coherence during the process is essential for a dynamical energetic behavior [105].


[1] R. Landauer, Information is physical, Phys. Today **44**(5), 23 (1991).

[2] R. Landauer, The physical nature of information, Phys. Lett. A **217**, 188 (1996).

[3] B. Groisman, S. Popescu, and A. Winter, Quantum, classical, and total amount of correlations in a quantum state, Phys. Rev. A **72**, 032317 (2005).

[4] M. Horodecki, P. Horodecki, R. Horodecki, J. Oppenheim, A. Sen, U. Sen, and B. Synak-Radtke, Local versus nonlocal information in quantum-information theory: Formalism and phenomena, Phys. Rev. A **71**, 062307 (2005).

[5] L. Rio, J. Åberg, R. Renner, O. Dahlsten, and V. Vedral, The thermodynamic meaning of negative entropy, Nature (London) **474**, 61 (2011).

[6] S. Deffner and C. Jarzynski, Information processing and the second law of thermodynamics: An inclusive, Hamiltonian approach, Phys. Rev. X **3**, 041003 (2013).

[7] A. C. Barato and U. Seifert, Stochastic thermodynamics with information reservoirs, Phys. Rev. E **90**, 042150 (2014).

[8] J. M. Horowitz and M. Esposito, Thermodynamics with continuous information flow, Phys. Rev. X **4**, 031015 (2014).

[9] P. Fadler, A. Friedenberger, and E. Lutz, Efficiency at maximum power of a Carnot quantum information engine, Phys. Rev. Lett. **130**, 240401 (2023).

[10] J. Ehrich and D. Sivak, Energy and information flows in autonomous systems, Front. Phys. **11**, 1108357 (2023).

[11] K. Maruyama, F. Nori, and V. Vedral, Colloquium: The physics of Maxwell's demon and information, Rev. Mod. Phys. **81**, 1 (2009).

[12] L. Szilard, On the decrease in entropy in a thermodynamic system by the intervention of intelligent beings, Z. Phys. **53**, 840 (1929).

[13] R. Landauer, Irreversibility and heat generation in the computing process, IBM J. Res. Dev. **5**, 183 (1961).

[14] J. Goold, M. Huber, A. Riera, L. del Rio, and P. Skrzypczyk, The role of quantum information in thermodynamics—A topical review, J. Phys. A: Math. Theor. **49**, 143001 (2016).

[15] J. Parrondo, J. Horowitz, and T. Sagawa, Thermodynamics of information, Nat. Phys. **11**, 131 (2015).

[16] H.-P. Breuer and F. Petruccione, *The Theory of Open Quantum Systems* (Oxford University Press, Oxford, 2002).

[17] G. Manzano, G. Kardeş, É. Roldán, and D. H. Wolpert, Thermodynamics of computations with absolute irreversibility, unidirectional transitions, and stochastic computation times, Phys. Rev. X **14**, 021026 (2024).

[18] J. Gea-Banacloche, Minimum energy requirements for quantum computation, Phys. Rev. Lett. **89**, 217901 (2002).

[19] M. Ozawa, Conservative quantum computing, Phys. Rev. Lett. **89**, 057902 (2002).

[20] A. Auffèves, Quantum technologies need a quantum energy initiative, PRX Quantum **3**, 020101 (2022).

[21] X. Linpeng, L. Bresque, M. Maffei, A. N. Jordan, A. Auffèves, and K. W. Murch, Energetic cost of measurements using quantum, coherent, and thermal light, Phys. Rev. Lett. **128**, 220506 (2022).

[22] J. Stevens, D. Szombati, M. Maffei, C. Elouard, R. Assouly, N. Cottet, R. Dassonneville, Q. Ficheux, S. Zeppetzauer, A. Bienfait, A. N. Jordan, A. Auffèves, and B. Huard, Energetics of a single qubit gate, Phys. Rev. Lett. **129**, 110601 (2022).

[23] I. Maillette de Buy Wenniger, S. E. Thomas, M. Maffei, S. C. Wein, M. Pont, N. Belabas, S. Prasad, A. Harouri, A. Lemaître, I. Sagnes, N. Somaschi, A. Auffèves, and P. Senellart, Experimental analysis of energy transfers between a quantum emitter and light fields, Phys. Rev. Lett. **131**, 260401 (2023).

[24] Elliott H. Lieb, Some convexity and subadditivity properties of entropy, in *Inequalities: Selecta of Elliott H. Lieb*, edited by Michael Loss and Mary Beth Ruskai (Springer, Berlin, 2002), pp. 67–79.

[25] C. H. Bennett, The thermodynamics of computation—A review, Int. J. Theor. Phys. **21**, 905 (1982).

[26] G. T. Landi and M. Paternostro, Irreversible entropy production: From classical to quantum, Rev. Mod. Phys. **93**, 035008 (2021).

[27] M. Esposito, K. Lindenberg, and C. Van den Broeck, Entropy production as correlation between system and reservoir, New J. Phys. **12**, 013013 (2010).

[28] S. W. Kim, T. Sagawa, S. De Liberato, and M. Ueda, Quantum Szilard engine, Phys. Rev. Lett. **106**, 070401 (2011).

[29] H. Dong, D. Z. Xu, C. Y. Cai, and C. P. Sun, Quantum Maxwell's demon in thermodynamic cycles, Phys. Rev. E **83**, 061108 (2011).

[30] C. Y. Cai, H. Dong, and C. P. Sun, Multiparticle quantum Szilard engine with optimal cycles assisted by a Maxwell's demon, Phys. Rev. E **85**, 031114 (2012).

[31] D. Reeb and M. Wolf, An improved Landauer principle with finite-size corrections, New J. Phys. **16**, 103011 (2014).

[32] S. Lorenzo, R. McCloskey, F. Ciccarello, M. Paternostro, and G. M. Palma, Landauer's principle in multipartite open quantum system dynamics, Phys. Rev. Lett. **115**, 120403 (2015).

[33] J. Goold, M. Paternostro, and K. Modi, Nonequilibrium quantum Landauer principle, Phys. Rev. Lett. **114**, 060602 (2015).

[34] K. Proesmans, J. Ehrich, and J. Bechhoefer, Finite-time Landauer principle, Phys. Rev. Lett. **125**, 100602 (2020).

[35] T. Van Vu and K. Saito, Finite-time quantum Landauer principle and quantum coherence, Phys. Rev. Lett. **128**, 010602 (2022).

[36] H. J. D. Miller, G. Guarnieri, M. T. Mitchison, and J. Goold, Quantum fluctuations hinder finite-time information erasure near the Landauer limit, Phys. Rev. Lett. **125**, 160602 (2020).

[37] J. Bengtsson, M. N. Tengstrand, A. Wacker, P. Samuelsson, M. Ueda, H. Linke, and S. M. Reimann, Quantum Szilard engine with attractively interacting bosons, Phys. Rev. Lett. **120**, 100601 (2018).

[38] J. Klaers, Landauer's erasure principle in a squeezed thermal memory, Phys. Rev. Lett. **122**, 040602 (2019).

[39] A. M. Timpanaro, J. P. Santos, and G. T. Landi, Landauer's principle at zero temperature, Phys. Rev. Lett. **124**, 240601 (2020).

[40] N. Freitas and M. Esposito, Maxwell demon that can work at macroscopic scales, Phys. Rev. Lett. **129**, 120602 (2022).

[41] A. Kolchinsky and D. H. Wolpert, Work, entropy production, and thermodynamics of information under protocol constraints, Phys. Rev. X **11**, 041024 (2021).

[42] A. B. Boyd, D. Mandal, and J. P. Crutchfield, Thermodynamics of modularity: Structural costs beyond the Landauer bound, Phys. Rev. X **8**, 031036 (2018).

[43] J. Koski, V. Maisi, J. Pekola, and D. Averin, Experimental realization of a Szilard engine with a single electron, Proc. Natl. Acad. Sci. USA **111**, 13786 (2014).

[44] J. Peterson, R. Sarthour, A. Souza, I. Oliveira, J. Goold, K. Modi, D. Soares-Pinto, and L. Céleri, Experimental demonstration of information to energy conversion in a quantum system at the Landauer limit, Proc. R. Soc. A **472**, 20150813 (2016).

[45] N. Cottet, S. Jezouin, L. Bretheau, P. Campagne-Ibarcq, Q. Ficheux, J. Anders, A. Auffèves, R. Azouit, P. Rouchon, and B. Huard, Observing a quantum maxwell demon at work, Proc. Natl. Acad. Sci. USA **114**, 7561 (2017).

[46] R. Gaudenzi, E. Burzurí, S. Maegawa, H. van der Zant, and F. Luis, Quantum Landauer erasure with a molecular nanomagnet, Nat. Phys. **14**, 565 (2018).

[47] L. L. Yan, T. P. Xiong, K. Rehan, F. Zhou, D. F. Liang, L. Chen, J. Q. Zhang, W. L. Yang, Z. H. Ma, and M. Feng, Single-atom demonstration of the quantum Landauer principle, Phys. Rev. Lett. **120**, 210601 (2018).

[48] M. Ribezzi-Crivellari and F. Ritort, Large work extraction and the Landauer limit in a continuous Maxwell demon, Nat. Phys. **15**, 660 (2019).

[49] G. Paneru and H. Pak, Colloidal engines for innovative tests of information thermodynamics, Adv. Phys.: X **5**, 1823880 (2020).

[50] M. O. Scully, M. S. Zubairy, G. S. Agarwal, and H. Walther, Extracting work from a single heat bath via vanishing quantum coherence, Science **299**, 862 (2003).

[51] R. Dillenschneider and E. Lutz, Energetics of quantum correlations, Europhys. Lett. **88**, 50003 (2009).

[52] J. Roßnagel, O. Abah, F. Schmidt-Kaler, K. Singer, and E. Lutz, Nanoscale heat engine beyond the Carnot limit, Phys. Rev. Lett. **112**, 030602 (2014).

[53] X. L. Huang, Tao Wang, and X. X. Yi, Effects of reservoir squeezing on quantum systems and work extraction, Phys. Rev. E **86**, 051105 (2012).

[54] G. Manzano, F. Galve, R. Zambrini, and J. M. R. Parrondo, Entropy production and thermodynamic power of the squeezed thermal reservoir, Phys. Rev. E **93**, 052120 (2016).

[55] W. Niedenzu, D. Gelbwaser-Klimovsky, A. Kofman, and G. Kurizki, On the operation of machines powered by quantum non-thermal baths, New J. Phys. **18**, 083012 (2016).

[56] S. Krishnamurthy, S. Ghosh, D. Chatterji, R. Ganapathy, and A. Sood, A micrometre-sized heat engine operating between bacterial reservoirs, Nat. Phys. **12**, 1134 (2016).

[57] C. L. Latune, I. Sinayskiy, and F. Petruccione, Quantum coherence, many-body correlations, and non-thermal effects for autonomous thermal machines, Sci. Rep. **9**, 3191 (2019).

[58] G. De Chiara and M. Antezza, Quantum machines powered by correlated baths, Phys. Rev. Res. **2**, 033315 (2020).

[59] R. Román-Ancheyta, B. Çakmak, and Ö. Müstecaplıoğlu, Spectral signatures of non-thermal baths in quantum thermalization, Quantum Sci. Technol. **5**, 015003 (2019).

[60] W. Ji, Z. Chai, M. Wang, Y. Guo, X. Rong, F. Shi, C. Ren, Y. Wang, and J. Du, Spin quantum heat engine quantified by quantum steering, Phys. Rev. Lett. **128**, 090602 (2022).

[61] Y. Lin, J. P. Gaebler, F. Reiter, T. R. Tan, R. Bowler, A. S. Sørensen, D. Leibfried, and D. J. Wineland, Dissipative production of a maximally entangled steady state of two quantum bits, Nature (London) **504**, 415 (2013).

[62] S. Shankar, M. Hatridge, Z. Leghtas, K. M. Sliwa, A. Narla, U. Vool, S. M. Girvin, L. Frunzio, M. Mirrahimi, and M. H. Devoret, Autonomously stabilized entanglement between two superconducting quantum bits, Nature (London) **504**, 419 (2013).

[63] N. Roy, N. Leroux, A. K. Sood, and R. Ganapathy, Tuning the performance of a micrometer-sized Stirling engine through reservoir engineering, Nat. Commun. **12**, 4927 (2021).

[64] M. Joos, D. Bluvstein, Y. Lyu, D. Weld, and A. Bleszynski Jayich, Protecting qubit coherence by spectrally engineered driving of the spin environment, npj Quantum Inf. **8**, 47 (2022).

[65] J. M. Kitzman, J. R. Lane, C. Undershute, P. M. Harrington, N. R. Beysengulov, C. A. Mikolas, K. W. Murch, and J. Pollanen, Phononic bath engineering of a superconducting qubit, Nat. Commun. **14**, 3910 (2023).

[66] P. Harrington, E. Mueller, and K. W. Murch, Engineered dissipation for quantum information science, Nat. Rev. Phys. **4**, 660 (2022).

[67] X. Mi, A. A. Michailidis, S. Shabani, K. C. Miao, P. V. Klimov, J. Lloyd, E. Rosenberg, R. Acharya, I. Aleiner, T. I. Andersen *et al.*, Stable quantum-correlated many body states through engineered dissipation, Science **383**, 1332 (2024).

[68] K. Ptaszyński and M. Esposito, Thermodynamics of quantum information flows, Phys. Rev. Lett. **122**, 150603 (2019).

[69] A. Bérut, A. Arakelyan, A. Petrosyan, S. Ciliberto, R. Dillenschneider, and E. Lutz, Experimental verification of Landauer's principle linking information and thermodynamics, Nature (London) **483**, 187 (2012).

[70] O.-P. Saira, M. H. Matheny, R. Katti, W. Fon, G. Wimsatt, J. P. Crutchfield, S. Han, and M. L. Roukes, Nonequilibrium thermodynamics of erasure with superconducting flux logic, Phys. Rev. Res. **2**, 013249 (2020).

[71] J. Åberg, Truly work-like work extraction via a single-shot analysis, Nat. Commun. **4**, 1925 (2013).

[72] G. Wimsatt, O. P. Saira, A. B. Boyd, M. H. Matheny, S. Han, M. L. Roukes, and J. P. Crutchfield, Harnessing fluctuations in thermodynamic computing via time-reversal symmetries, Phys. Rev. Res. **3**, 033115 (2021).

[73] M. Esposito, U. Harbola, and S. Mukamel, Nonequilibrium fluctuations, fluctuation theorems, and counting statistics in quantum systems, Rev. Mod. Phys. **81**, 1665 (2009).

[74] U. Seifert, Stochastic thermodynamics, fluctuation theorems and molecular machines, Rep. Prog. Phys. **75**, 126001 (2012).

[75] S. Deffner, J. P. Paz, and W. H. Zurek, Quantum work and the thermodynamic cost of quantum measurements, Phys. Rev. E **94**, 010103(R) (2016).

[76] A. Sone, Y.-X. Liu, and P. Cappellaro, Quantum Jarzynski equality in open quantum systems from the one-time measurement scheme, Phys. Rev. Lett. **125**, 060602 (2020).

[77] K. Beyer, K. Luoma, and W. T. Strunz, Work as an external quantum observable and an operational quantum work fluctuation theorem, Phys. Rev. Res. **2**, 033508 (2020).

[78] K. Mølmer, Y. Castin, and J. Dalibard, Monte Carlo wavefunction method in quantum optics, J. Opt. Soc. Am. B **10**, 524 (1993).

[79] M. Plenio and P. Knight, The quantum-jump approach to dissipative dynamics in quantum optics, Rev. Mod. Phys. **70**, 101 (1998).

[80] T. Becker, C. Netzer, and A. Eckardt, Quantum trajectories for time-local non-Lindblad master equations, Phys. Rev. Lett. **131**, 160401 (2023).

[81] W. Cheng, W. Liu, Y. Wu, Z. Niu, C. K. Duan, J. Gong, X. Rong, and J. Du, Experimental study on the principle of minimal work fluctuations, Phys. Rev. A **108**, 042423 (2023).

[82] O. Dahlsten, R. Renner, E. Rieper, and V. Vedral, Inadequacy of von Neumann entropy for characterizing extractable work, New J. Phys. **13**, 053015 (2011).

[83] E. Jaynes, Information theory and statistical mechanics, Phys. Rev. **106**, 620 (1957).

[84] P. Strasberg and A. Winter, First and second law of quantum thermodynamics: A consistent derivation based on a microscopic definition of entropy, PRX Quantum **2**, 030202 (2021).

[85] R. Alicki and M. Fannes, Entanglement boost for extractable work from ensembles of quantum batteries, Phys. Rev. E **87**, 042123 (2013).

[86] C. Sparaciari, D. Jennings, and J. Oppenheim, Energetic instability of passive states in thermodynamics, Nat. Commun. **8**, 1895 (2017).

[87] M. Bera, A. Riera, M. Lewenstein, Z. Khanian, and A. Winter, Thermodynamics as a consequence of information conservation, Quantum **3**, 121 (2019).

[88] C. Elouard and C. Lombard Latune, Extending the laws of thermodynamics for arbitrary autonomous quantum systems, PRX Quantum **4**, 020309 (2023).
[89] J. Liu and H. Nie, Universal Landauer-like inequality from the first law of thermodynamics, Phys. Rev. A **108**, L040203 (2023).
[90] B. Gardas and S. Deffner, Thermodynamic universality of quantum Carnot engines, Phys. Rev. E **92**, 042126 (2015).
[91] J. Liu, K. A. Jung, and D. Segal, Periodically driven quantum thermal machines from warming up to limit cycle, Phys. Rev. Lett. **127**, 200602 (2021).
[92] J. Liu and K. A. Jung, Quantum Carnot thermal machines reexamined: Definition of efficiency and the effects of strong coupling, Phys. Rev. E **109**, 044118 (2024).
[93] J. S. Lee, S. Lee, H. Kwon, and H. Park, Speed limit for a highly irreversible process and tight finite-time Landauer's bound, Phys. Rev. Lett. **129**, 120603 (2022).
[94] T. Sagawa and M. Ueda, Second law of thermodynamics with discrete quantum feedback control, Phys. Rev. Lett. **100**, 080403 (2008).
[95] K. Jacobs, Second law of thermodynamics and quantum feedback control: Maxwell's demon with weak measurements, Phys. Rev. A **80**, 012322 (2009).
[96] J. Parrondo, J. Tabanera-Bravo, F. Fedele, and N. Ares, Information flows in nanomachines, arXiv:2312.02068.
[97] Noting that if the heat dissipation also vanishes as $T_E \to 0$, it is then inappropriate to state that the Landauer bound has a trivial zero temperature limit.
[98] A. C. Barato and U. Seifert, Thermodynamic uncertainty relation for biomolecular processes, Phys. Rev. Lett. **114**, 158101 (2015).
[99] T. R. Gingrich, J. M. Horowitz, N. Perunov, and J. L. England, Dissipation bounds all steady-state current fluctuations, Phys. Rev. Lett. **116**, 120601 (2016).
[100] J. Horowitz and T. Gingrich, Thermodynamic uncertainty relations constrain non-equilibrium fluctuations, Nat. Phys. **16**, 15 (2020).
[101] B. K. Agarwalla and D. Segal, Assessing the validity of the thermodynamic uncertainty relation in quantum systems, Phys. Rev. B **98**, 155438 (2018).
[102] J. Liu and D. Segal, Thermodynamic uncertainty relation in quantum thermoelectric junctions, Phys. Rev. E **99**, 062141 (2019).
[103] T. Baumgratz, M. Cramer, and M. B. Plenio, Quantifying coherence, Phys. Rev. Lett. **113**, 140401 (2014).
[104] G. Francica, J. Goold, and F. Plastina, Role of coherence in the nonequilibrium thermodynamics of quantum systems, Phys. Rev. E **99**, 042105 (2019).
[105] T. Ma, M. J. Zhao, S. M. Fei, and M. H. Yung, Necessity for quantum coherence of nondegeneracy in energy flow, Phys. Rev. A **99**, 062303 (2019).
[106] H. M. Wiseman, Quantum theory of continuous feedback, Phys. Rev. A **49**, 2133 (1994).
[107] J.-H. Jiang and Y. Imry, Linear and nonlinear mesoscopic thermoelectric transport with coupling with heat baths, C. R. Phys. **17**, 1047 (2016).
[108] R. Wang, C. Wang, J. Lu, and J.-H. Jiang, Inelastic thermoelectric transport and fluctuations in mesoscopic systems, Adv. Phys.: X **7**, 2082317 (2022).
[109] J. Lu, Z. Wang, J. Peng, C. Wang, J. H. Jiang, and J. Ren, Geometric thermodynamic uncertainty relation in a periodically driven thermoelectric heat engine, Phys. Rev. B **105**, 115428 (2022).
[110] J. Lu, Z. Wang, J. Ren, C. Wang, and J.-H. Jiang, Coherence-enhanced thermodynamic performance in a periodically driven inelastic heat engine, Phys. Rev. B **109**, 125407 (2024).
[111] J.-H. Jiang, O. Entin-Wohlman, and Y. Imry, Thermoelectric three-terminal hopping transport through one-dimensional nanosystems, Phys. Rev. B **85**, 075412 (2012).
[112] J. Lu, Z. Wang, R. Wang, J. Peng, C. Wang, and J.-H. Jiang, Multitask quantum thermal machines and cooperative effects, Phys. Rev. B **107**, 075428 (2023).
[113] A. Grankin, E. Brion, E. Bimbard, R. Boddeda, I. Usmani, A. Ourjoumtsev, and P. Grangier, Quantum statistics of light transmitted through an intracavity Rydberg medium, New J. Phys. **16**, 043020 (2014).
[114] M. B. Plenio, S. F. Huelga, A. Beige, and P. L. Knight, Cavity-loss-induced generation of entangled atoms, Phys. Rev. A **59**, 2468 (1999).
[115] B. Kraus, H. P. Büchler, S. Diehl, A. Kantian, A. Micheli, and P. Zoller, Preparation of entangled states by quantum Markov processes, Phys. Rev. A **78**, 042307 (2008).
[116] S. Diehl, A. Micheli, A. Kantian, B. Kraus, H. P. Büchler, and P. Zoller, Quantum states and phases in driven open quantum systems with cold atoms, Nat. Phys. **4**, 878 (2008).
[117] F. Verstraete, M. Wolf, and J. I. Cirac, Quantum computation and quantum-state engineering driven by dissipation, Nat. Phys. **5**, 633 (2009).
[118] Z. Leghtas, U. Vool, S. Shankar, M. Hatridge, S. M. Girvin, M. H. Devoret, and M. Mirrahimi, Stabilizing a Bell state of two superconducting qubits by dissipation engineering, Phys. Rev. A **88**, 023849 (2013).
[119] M. J. Kastoryano, F. Reiter, and A. S. Sørensen, Dissipative preparation of entanglement in optical cavities, Phys. Rev. Lett. **106**, 090502 (2011).
[120] Z. Leghtas, S. Touzard, I. M. Pop, A. Kou, B. Vlastakis, A. Petrenko, K. M. Sliwa, A. Narla, S. Shankar, M. J. Hatridge, M. Reagor, L. Frunzio, R. J. Schoelkopf, M. Mirrahimi, and M. H. Devoret, Confining the state of light to a quantum manifold by engineered two-photon loss, Science **347**, 853 (2015).
[121] D. Kienzler, H.-Y. Lo, B. Keitch, L. de Clercq, F. Leupold, F. Lindenfelser, M. Marinelli, V. Negnevitsky, and J. P. Home, Quantum harmonic oscillator state synthesis by reservoir engineering, Science **347**, 53 (2015).
[122] D. X. Li and X. Q. Shao, Unconventional Rydberg pumping and applications in quantum information processing, Phys. Rev. A **98**, 062338 (2018).
[123] J. P. Santos, G. T. Landi, and M. Paternostro, Wigner entropy production rate, Phys. Rev. Lett. **118**, 220601 (2017).
[124] C. Koch, Controlling open quantum systems: Tools, achievements, and limitations, J. Phys.: Condens. Matter **28**, 213001 (2016).
[125] H. Y. Huang, S. Chen, and J. Preskill, Learning to predict arbitrary quantum processes, PRX Quantum **4**, 040337 (2023).
[126] S. Nandy, M. Schmitt, M. Bukov, and Z. Lenarčič, Reconstructing effective Hamiltonians from nonequilibrium thermal

and prethermal steady states, Phys. Rev. Res. **6**, 023160 (2024).

[127] Isaac L. Chuang and M. A. Nielsen, Prescription for experimental determination of the dynamics of a quantum black box, J. Mod. Opt. **44**, 2455 (1997).

[128] K. Siva, G. Koolstra, J. Steinmetz, W. P. Livingston, D. Das, L. Chen, J. M. Kreikebaum, N. J. Stevenson, C. Jünger, D. I. Santiago, I. Siddiqi, and A. N. Jordan, Time-dependent Hamiltonian reconstruction using continuous weak measurements, PRX Quantum **4**, 040324 (2023).

[129] E. Crosson and D. Lidar, Prospects for quantum enhancement with diabatic quantum annealing, Nat. Rev. Phys. **3**, 466 (2021).

[130] A. Callison, M. Festenstein, J. Chen, L. Nita, V. Kendon, and N. Chancellor, Energetic perspective on rapid quenches in quantum annealing, PRX Quantum **2**, 010338 (2021).